



HAL
open science

Terminal differentiation of goat mammary tissue during pregnancy requires the expression of genes involved in immune functions

Felicie Faucon, Emmanuelle Rebours, Claudia Bevilacqua, Jean-Christophe Helbling, Julie Aubert, Samira Makhzami, Sophie Pollet, Stephane Robin, Patrice Martin

► To cite this version:

Felicie Faucon, Emmanuelle Rebours, Claudia Bevilacqua, Jean-Christophe Helbling, Julie Aubert, et al.. Terminal differentiation of goat mammary tissue during pregnancy requires the expression of genes involved in immune functions. *Physiological Genomics*, 2009, 40 (1), pp.61-82. hal-01193417

HAL Id: hal-01193417

<https://hal.science/hal-01193417>

Submitted on 30 May 2020

HAL is a multi-disciplinary open access archive for the deposit and dissemination of scientific research documents, whether they are published or not. The documents may come from teaching and research institutions in France or abroad, or from public or private research centers.

L'archive ouverte pluridisciplinaire **HAL**, est destinée au dépôt et à la diffusion de documents scientifiques de niveau recherche, publiés ou non, émanant des établissements d'enseignement et de recherche français ou étrangers, des laboratoires publics ou privés.

Terminal differentiation of goat mammary tissue during pregnancy requires the expression of genes involved in immune functions

F. Faucon,^{1,2} E. Rebours,¹ C. Bevilacqua,¹ J.-C. Helbling,¹ J. Aubert,³ S. Makhzami,¹ S. Dhorne-Pollet,¹ S. Robin,³ and P. Martin¹

¹Institut National de la Recherche Agronomique (INRA), Unité Mixte de Recherche (UMR) 1313, Génétique animale et Biologie intégrative, équipe LGS, Jouy-en-Josas; ²Institut de l'Élevage; and ³UMR Institut National Agronomique Paris-Grignon/Ecole Nationale du Génie Rural, des Eaux et des Forêts/INRA 518, Mathématiques et Informatique Appliquées, Paris, France

Submitted 6 February 2009; accepted in final form 12 October 2009

Faucon F, Rebours E, Bevilacqua C, Helbling J-C, Aubert J, Makhzami S, Dhorne-Pollet S, Robin S, Martin P. Terminal differentiation of goat mammary tissue during pregnancy requires the expression of genes involved in immune functions. *Physiol Genomics* 40: 61–82, 2009. First published October 20, 2009; doi:10.1152/physiolgenomics.00032.2009.—Terminal differentiation of mammary tissue into a functional epithelium that synthesizes and secretes milk occurs during pregnancy. The molecular mechanisms underlying this complex process are poorly understood, especially in ruminants. To obtain an overview of the ruminant mammary gland's final differentiation process, we conducted time-course gene expression analysis of five physiological stages: four during pregnancy (P46, P70, P90, and P110) and one after 40 days of lactation (L40). An appropriate loop experimental design was used to follow gene expression profiles. Using three nulliparous (pregnancy) or primiparous (lactation) goats per stage, we performed a comparison starting from nine dye-swaps and using a 22K bovine oligoarray. Statistical analysis revealed that the expression of 1,696 genes varied significantly at least once in the study. These genes fell into 19 clusters based on their expression profiles. Identification of biological functions with Ingenuity Pathway Analysis software revealed several similarities, in keeping with physiological stages described in mice. As in mice, expression of milk protein genes began at midpregnancy, and genes regulating lipid biosynthesis were induced at the onset of lactation. During the first half of pregnancy, the molecular signature of goat mammary tissue was characterized by the expression of genes associated with tissue remodeling and differentiation, while the second half was mainly characterized by the presence of messengers encoding genes involved in cell proliferation. A large number of immune-related genes were also induced, supporting recent speculation that mammary tissue has an original immune function, and the recruitment of migrating hematopoietic cells possibly involved in the branching morphogenesis of the mammary gland. These data hint that the induction of differentiation occurs early in pregnancy, very likely before P46. This period is therefore crucial for obtaining a healthy and productive mammary gland.

development; mammary gland; ruminants; gene expression profiling; innate and specific immunity

MORPHOLOGICAL DEVELOPMENT of the mammary gland begins during embryonic life with the majority of development and differentiation occurring postnatally. Isometric growth occurs in the early postnatal period followed by allometric growth phases during the prepubertal/pubertal period of mammary development in ruminant females. With the onset of pregnancy

the mammary gland commences another round of allometric growth (25). Terminal differentiation of mammary tissue into an epithelium capable of synthesizing and secreting milk occurs only during pregnancy and is under the control of multiple hormones and paracrine factors. Progesterone, first synthesized by the ovarian corpus luteum in early pregnancy, is mainly produced by the placenta after the first third of pregnancy in women (39) and small ruminants. In the mammary gland, both steroid hormones, progesterone and estrogen, control ductal outgrowth and lobulo-alveolar expansion. Systemic effects of these hormones and interactions between their signaling pathways make the determination of their individual roles difficult. Estrogen might be a critical mediator of mammary epithelial cell (MEC) proliferation, whereas progesterone would be a stimulator of lobulo-alveolar differentiation in the pregnant gland (17). Prolactin, a pituitary hormone, triggers lactation and is essential for its maintenance. In addition it plays a crucial role in the early stage of alveolar proliferation, in mice, before apparently being replaced by placental hormones (39). Placental lactogen hormone is activated in late pregnancy and is involved in goat mammary gland development by inducing alveolar epithelial cell differentiation and proliferation (2, 22). Cortisol, the main bovine glucocorticoid, stimulates lobulo-alveolar differentiation at parturition (60). It was recently reported that IGF-1, a local factor secreted by the stroma and/or adipocytes, after activation by growth hormone (GH), participates in epithelial cell proliferation in heifer mammary tissue (17). Some other local factors, well described in mice and involved in mammary gland and alveolar development, such as RANKL (receptor activator of nuclear factor κ B-ligand), inhibin β , TGF- β (transforming growth factor- β), cyclin D1, A-myb, and C/EBP- β (CAAT enhancer binding protein- β), are synthesized by epithelial cells, as well as in the stroma (reviewed in Refs. 22, 23).

After puberty, rodent mammary glands are composed of many branched ducts ending in terminal end buds (TEB) and surrounded by a mammary fat pad (24, 25). In rodents, lobulo-alveolar growth occurs during the first third of pregnancy. The last (second) half of pregnancy is characterized by differentiation and a reduced rate of alveolar proliferation (23, 44). Secretory activation, which is the ultimate step of mammary gland differentiation, occurs only at parturition and is characterized by the expression of genes involved in lipid and lactose biosynthesis (4, 49). By contrast, there is significant expression of caseins and/or α -lactalbumin (mRNA and proteins) in mid-pregnancy mammary tissue (27, 37, 47, 49).

Address for reprint requests and other correspondence: P. Martin, INRA, Génétique animale et Biologie intégrative, F-78352 Jouy-en-Josas, France (e-mail: patrice.martin@jouy.inra.fr).

At the beginning of pregnancy, the ruminant mammary gland is made up of an epithelium associated with fibroblastic connective tissue and relatively few lipid-filled adipocytes (24). The mammary gland is structured by a cistern, a primary duct that branches into secondary and tertiary ducts. Clusters of ductules form so-called terminal ductule lobular units (TDLU) (1, 24, 25). Differentiation of ruminant mammary gland into a secretory tissue during pregnancy has not been described in detail. Only one morphological description of bovine mammary development and differentiation has been reported, 30 years ago by Swanson and Poffenbarger (59). These authors showed that bovine mammary tissue already has visible lobuloalveolar structures (LAS) in midpregnancy and that these structures contain some secretory material. The mammary parenchyma develops continuously. At parturition, the secretory LAS are fully developed and occupy the entire mammary space. They contain more defined secretory material (fat globules and casein micelles). The latest studies of ruminant mammary gland development and differentiation date back more than 25 years (3). They show that mammary gland weight and DNA and RNA levels increase during pregnancy, reflecting an increase in cellular activity. Enzymatic activity increases in bovine mammary tissue several weeks before the initiation of lactation (6). Moreover, the activities of enzyme involved in lactose and fatty acid synthesis increase between 7 days prepartum and 7 days postpartum (34).

Much work has been done in recent years on mouse mammary gland development, including gene expression profiling experiments (16, 32, 38, 49). By contrast there are very few descriptions of general mechanisms and biological changes underlying ruminant mammary gland terminal differentiation during pregnancy. A first microarray analysis of cow mammary tissue shows that 16 genes are preferentially expressed during mammary gland development (57). More recently, the transition from late pregnancy to lactation (secretory switch) was shown to be characterized by downregulation of genes encoding cell proliferation factors and upregulation of genes involved in milk synthesis (20). To unravel the network of genes that participate in coordinating milk fat synthesis and secretion, Bionaz and Looor (9) quantified the expression of 45 relevant genes from the late prepartum/nonlactating period through the end of subsequent lactation. Elsewhere, expression patterns of genes that can alter mammary tissue sensitivity to galactopoietic thyroid hormones have been evaluated during the last 50 days before expected parturition and during the first weeks of lactation (11). However, global analyses of gene expression in ruminant mammary tissue at different points of the final differentiation process are lacking.

Here we report the identification of genes whose expression changes during terminal differentiation of goat mammary tissue. In addition, we used oligoarrays for gene expression profiling and longitudinal mRNA expression analysis during the course of pregnancy in an attempt to unravel gene networks and further understand the mechanisms by which goat mammary tissue acquires its secretory phenotype. Our results strongly suggest that mammary gland terminal differentiation during pregnancy, which is a period of intensive tissue remodeling, also requires, as demonstrated for involution (5, 16, 56), the expression of immune-related genes.

MATERIALS AND METHODS

Animals and tissue sampling. Pregnant or primiparous lactating Saanen or Alpine goats from an INRA experimental farm (UE325, UCEA Brouessy, Magny-Les-Hameaux, France), were euthanized, immediately after milking, in safe and painless conditions, in compliance with the INRA Animal Care Committee guidelines. At slaughter, mammary glands were removed quickly (within 2–3 min), and pieces (5–10 g) of mammary parenchymal tissue were carefully taken for isolation of RNA, under sterile conditions, in a zone located in the middle of the parenchymal area, excluding peripheric stromal tissue. Approximately 1-cm³ tissue blocks were washed in ice-cold saline to remove residual milk and then immediately frozen into liquid nitrogen and stored at –80°C until further processing. We studied five different developmental stages of mammary epithelium, hereafter called “time points,” corresponding to 46, 70, 90, and 110 days of pregnancy and 40 days of lactation and designated P46, P70, P90, P110, and L40, respectively. Given parenchymal mammary tissue was scarce and highly heterogeneous in early pregnancy (P46), no morphological and/or biochemical controls for tissue type collected were performed. Mammary glands from three different goats were used to characterize each stage of pregnancy or lactation, to reduce the impact of individual variability.

RNA extraction. Frozen mammary tissue samples were ground in liquid nitrogen with a Freezer Mill 6750 (Fisher Scientific Bioblock). Total RNA was extracted by mixing the resulting powder with TRIzol reagent following the manufacturer’s instructions (Invitrogen, Cergy-Pontoise, France). The resulting aqueous phase of each sample was purified on QIAGEN RNeasy mini-columns. After DNaseI treatment (Qiagen SA, Courtaboeuf, France) total RNA was eluted and concentration was determined as the 260/280 nm OD ratio with a Nanodrop ND-1000 spectrophotometer (Nanodrop Technology, Nyxor Biotech). The quality of each RNA sample was evaluated on an Agilent 2100 Bioanalyzer with 6000 Nano LabChip kits (Agilent Technologies). Samples with an RNA integrity number (RIN) factor (52) <7.5 were discarded.

RNA labeling. RNA samples were labeled using the Superscript Plus Indirect cDNA labeling protocol (Invitrogen) according to the manufacturer’s instructions. Briefly, 10 µg of total RNA was first reverse transcribed using SuperScript III Reverse Transcriptase and converted into aminoallyl cDNAs, which were separated from non-incorporated amino-modified dNTPs on S.N.A.P. columns. They were then labeled with Cy3 or Cy5 dyes (Amersham Bioscience, GE Healthcare Europe, Saclay, France) and subsequently separated from non-incorporated dyes on S.N.A.P. columns. Frequencies of dye incorporation (FOI, rate per thousand labeled nucleotides) and cDNA concentrations were estimated for both dyes by measuring the absorbance at 260 nm, 550 nm and 650 nm on a Nanodrop spectrophotometer (Nyxor Biotech). The following ratios were calculated: FOI (Cy3) = (Abs550 × 324.5)/(Abs260 × 5.55), FOI (Cy5) = (Abs650 × 324.5)/(Abs260 × 9.25) and an upper limit of 20 was chosen to retain labeled cDNA samples for further analysis. Cyanine incorporation was finally checked by scanning, with a Typhoon 9410 imager (GE Healthcare), 1% agarose gels on which fluorescently labeled cDNAs had been resolved by electrophoresis.

Microarray processing and data analysis. Since goat microarrays were not available, we used a heterologous system, i.e., an oligoarray developed for a closely related species (bovine), for gene expression profiling. Such an approach has already been successfully used to study the impact of different genotypes occurring at the CSN1S1 locus (encoding α_{s1} -casein) on the goat mammary transcriptome (42). Microarrays used in this study were 22K bovine oligonucleotide probe arrays [National Center for Biotechnology Information (NCBI) Gene Expression Omnibus (GEO): 6694] spotted by Centre de Ressources Biologiques - Génomique des Animaux Domestiques et d’Intérêt Economique (CRB-GADIE, INRA, Jouy-en-Josas, France). Of the 23,232 probes spotted on the slides, 960 were empty spots, 260 were

spots containing buffer, 8,709 spots were oligonucleotides from the Bovine Genome Oligoset V1.1 (Operon Biotechnologies), and 13,303 spots were oligonucleotides from a pre-existing set (NCBI GEO: GPL2853), developed from a bovine embryo cDNA library (19). These two bovine oligonucleotide sets are identified hereafter as “Operon” and “Illumina” sets, respectively.

Prior to hybridization, microarrays were prehybridized for 30 min at 50°C in a filtered solution of 1% BSA, 3.5× SSC, 0.1% SDS and rinsed twice in ultrapure water for 5 min with orbital agitation. Each microarray was cohybridized with two fluorescently labeled (Cy3 and Cy5) cDNA samples. An evaluated amount of 380 ng of each labeled cDNA was fragmented for 30 min at 60°C in 1× fragmentation buffer (Agilent Technologies). Then, fragmented labeled cDNA samples were diluted in Agilent hybridization buffer and hybridized on the 22K bovine oligoarray for 20 h at 60°C in a rotating hybridization oven (Agilent Technologies).

An even-loop experimental design (Fig. 1) was developed based on variance minimization (28, 29). In this experimental design, every time point was compared with the four others in nine dye-swaps, except for the comparison between the most distant time points (P46 and L40). One dye-swap corresponded to one comparison, meaning two slides.

After hybridization, microarrays were washed twice with orbital agitation for 5 min at 50°C in 2× SSC-0.1% SDS and were then successively washed twice at room temperature in (0.5× SSC, 0.1% SDS) solution for 5 min, (0.1× SSC, 0.1% SDS) solution for 5 min, (0.1× SSC) solution three times for 5 min, and in ultrapure water for 1 min. They were finally dried for 45 s in a minicentrifuge system.

Microarrays were scanned on an Agilent scanner (Agilent Technologies) at a 10 μm × 10 μm pixel resolution. Agilent Feature Extraction 9.1.3.1 software (Agilent Technologies) was used to quantify mean and median signals for each sample and for background estimation following the GE2_NonAgilent_91 extraction protocol. Extracted data were stored in the BioArray Software Environment (BASE) of SIGENAE (Système d’Information des GENomes des Animaux d’Elevage) 2008 (<http://www.sigenae.org>) and then formatted according to MIAME standards (10). The data have been submitted to

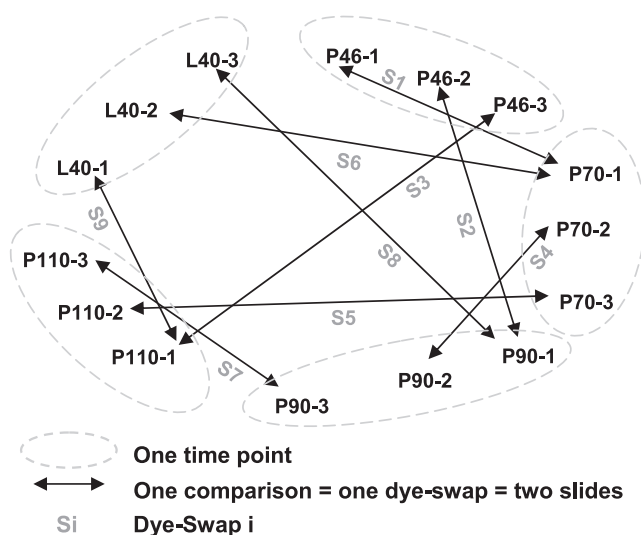
NCBI’s GEO database as series GSE14008 (<http://www.ncbi.nlm.nih.gov/geo/query/acc.cgi?token=jrqrhioqcywkmte&acc=GSE14008>), and were analyzed with R Program Writer software (<http://www.r-project.org/>).

Statistical analyses. Data were normalized using the “normalisation” function of the “anapuce” R package, based on an intensity-dependent procedure with a global lowess (64) followed by subtraction of the log-ratio median calculated over the values for an entire block from each individual log-ratio to correct for a possible print-tip effect.

First, we calculated the average normalized signal for each spot at every time point. The most strongly expressed genes were selected when the corresponding spot signal intensity represented, at a given time point, >10% of the most intense signal observed. Genes that were globally highly expressed at every time point were also selected.

In a second analysis, experimental normalized data extracted from the microarrays of dye-swaps S1, S4, S7, and S9 (Fig. 1) were compared between pairs of time points, as follows: P46 with P70 (P46/P70), P70 with P90 (P70/P90), P90 with P110 (P90/P110) and P110 with L40 (P110/L40), respectively. Differential analysis with variance mixture modeling (18), based on the “DiffAnalysis” function developed in the anapuce package of R, was performed on the normalized data set. This method builds up groups of genes with homogeneous variance. To take into account the multiplicity of tests, *P* values were adjusted with the Benjamini-Hochberg procedure (7) which controls the false discovery rate (FDR) with a significance threshold set at 5%.

In the third analysis, the entire data set was analyzed with a linear model that included a stage effect. We used the covariance matrix of the parameter estimates to calculate the variance of all contrasts between successive stages $\mu_{i+1} - \mu_i$ and assessed their significance with a *t*-test. *P* values were corrected with the Benjamini-Hochberg procedure (7). Genes whose expression varied significantly at least once during pregnancy and lactation were clustered using the KMC (K-means clustering) function of TMeV v4.0 software (51, 55). KMC was considered appropriate as it builds homogeneous clusters by characterizing each cluster with a central point (its mean), assigning



Dye-Swap	Slide	Time point in Cy3	Time point in Cy5
1	S1	P46	P70
	S2	P70	P46
2	S3	P46	P90
	S4	P90	P46
3	S5	P46	P110
	S6	P110	P46
4	S7	P70	P90
	S8	P90	P70
5	S9	P70	P110
	S10	P110	P70
6	S11	P70	L40
	S12	L40	P70
7	S13	P90	P110
	S14	P110	P90
8	S15	P90	L40
	S16	L40	P90
9	S17	P110	L40
	S18	L40	P110

Fig. 1. Loop experimental design and hybridization table. P, pregnancy; L, lactation.

each gene to the closest cluster, and recalculating the mean of the cluster (31). The parameters used to build the clusters were the Euclidean distance and a maximum of 50 iterations.

General slide information and probe annotation. To recover GenBank accession numbers and human references for each probe on the slide, we used a web-accessible resource established by SIGENAE (http://public-contigbrowser.sigenae.org:9090/Bos_taurus/index.html), selecting either Human Unigene or SwissProt filters. To annotate the probes in this contig browser (BioMart), the SIGENAE tool first compared the 70 mer oligonucleotide sequences spotted on the slide with the latest version of the bovine genome assembling (Cattle V8 s.bt.8 based on p.bt.5 published in November 2007). If the 70 mer oligonucleotide sequence matched the bovine assembling perfectly at a single place, then the annotation associated with this locus was directly selected to annotate the probe. If the match was imperfect, the 70 mer oligonucleotide sequence was compared with all Ensembl transcripts and the retained probe annotation corresponded to the contig number that contained the sequence.

Among the 22,012 oligonucleotide sequences spotted on the glass slides, 416 were control spots and 21,596 corresponded to different sequences. Among these 21,596 sequences, 14,687 (~68%) had a human reference accepted by Ingenuity Pathway Analysis software v6.0 (IPA, Ingenuity Systems, Redwood City, CA). Of these 14,687 "IPA genes," 4,714 (~32%) were redundant between the Operon and Illumina sets. In other words, with ~17,000 UniGene clusters (9,973 different genes analyzed in IPA and ~7,000 probes with Sigenae's annotation not accepted by IPA), the oligoarray platform used in this study represents a meaningful bovine gene repertoire.

Identification of biological functions. For each analysis, significant data were referenced to biological functions with IPA software. The contribution of genes to the identified function was explained with an associated *P* value, calculated with the right-tailed Fisher's exact test. In this test the number of user-specified genes of interest that participated in a given function or pathway was compared with the total number of occurrences of these genes in all functional/pathway annotations stored in the Ingenuity Pathways Knowledge Base. Only significant top IPA molecular and cellular functions and IPA physiological system development and functions (*P* value <5%) are presented and discussed in this article.

Primer design and quantitative real-time PCR. Total RNA (1 µg) was reversed transcribed with 0.5 µg of Oligo(dT)12–18 primer and SuperScript III (Invitrogen). The quantitative real-time PCR (qPCR) was carried out as described by Bevilacqua et al. (8), using the SYBR Green PCR Master mix and the ABI Prism 7900 Sequence Detection System (Applied Biosystems, Foster City, CA) to measure mRNA abundance. A total of 24 genes were validated by qPCR, using three potential reference genes, cyclophilin A, 18S ribosomal RNA and S24 ribosomal protein (RPS24), as internal controls. As previously reported (8), RPS24 mRNA was chosen as the internal control. Primer pairs shown in Table 1 were designed using Primer Express Applied Biosystems software v2.0 (Applied Biosystems, France), starting from publicly available caprine and bovine sequences. To avoid genomic DNA amplification, primers were primarily selected on exon-exon splice boundaries of goat messenger sequences, when available, or otherwise from bovine sequences. Primers were purchased from MWG Biotech (France).

All melt curves showed a single amplicon and the specificity of most of the qPCR assays was confirmed by amplicon sizing and sequencing. Amplification efficiency was measured for each system and differences in gene expression were analyzed using one-way ANOVA with a threshold of significance set at *P* < 0.01.

To compare the expression profile of selected genes in qPCR and microarray experiments, we first normalized (with RPS24 transcripts as internal control) individual qPCR data. Relative abundances of target transcripts at the different stages of pregnancy were determined, assuming the expression of individual lactation was 1,000. The same procedure was applied to microarray data, except that normalization

was performed as described above. Then the mean and standard deviation for each developmental stage were calculated and bar charts were drawn.

Preparation of thin mammary tissue sections for histology. For histological studies, dissected samples of mammary tissue, taken at the indicated time points, were washed immediately after collection in cold PBS, cut into cubes 3–4 mm thick, embedded in OCT (TissueTek), placed in cryomolds of 1 cm³ (Bayer) and immediately immersed in liquid nitrogen. Samples were stored at –80°C until further processing. Mammary tissue sections (8 µm) were obtained for histological analysis by using a cryostat (Thermo Shandon, France) and were then stained with hematoxylin for 30 s and dehydrated through a graded series of ethanol solutions: 1 min in 75% ethanol, twice 1 min in 95% ethanol, twice 1 min in 100% ethanol anhydrous (Fluka, Sigma-Aldrich, Lyon, France).

RESULTS

Three independent analyses of the microarray data were performed. In each we determined the most relevant *P* value based on experiments previously carried out in our laboratory (unpublished results) and the statistical methods used. The three independent analyses were the following: 1) extraction of the most highly expressed genes at each developmental stage, 2) identification of genes whose expression varied between two successive time points, and 3) clustering of genes sharing the same expression profile, from 46 days of pregnancy (P46) to 40 days of lactation (L40). In addition, expression profiles of relevant genes identified by microarray analyses were validated with qPCR.

The most highly expressed genes at each developmental stage. To obtain an overview of genes highly expressed at each developmental stage, we selected spots with signals >10% of the highest signal on each array. The number of highly expressed genes was relatively constant throughout pregnancy (Table 2), ranging between 130 (L40) and 175 (P90).¹

Eighty-two probes were common to all time points (Table 3). They corresponded to 48 different genes with known identifiers that mapped to their corresponding gene object in the Ingenuity Pathways Knowledge Base. These genes were overlaid onto a global molecular network built from information contained in the database. They were representative of the following molecular and cellular functions: cell cycling, cell morphology, posttranslational modification, cell death, and cell signaling. Some of these genes have been shown to be involved in apoptosis, such as BAX (BCL-2 associated X-protein), BCL-2 (B-cell leukemia/lymphoma 2) and STAT3 (signal transducer and activator of transcription 3), which were highly expressed at every developmental stage. They are known to participate in apoptosis and differentiation of macrophages. Other genes such as HMGAI (high mobility group AT-hook 1), ZAK (sterile alpha motif and leucine zipper containing kinase AZK) and EEF1A1 (eukaryotic translation elongation factor 1 α 1) that are regulators of transcription and translation also belonged to this set. Likewise, RHOC (ras homolog gene family, member C), which promotes reorganization of the actin cytoskeleton and regulates cell shape attachment and motility showed high signal intensity at every developmental stage. EGFL7 (EGF-like-domain, multiple 7), which behaved like-

¹ The online version of this article contains supplemental material.

Table 1. Oligonucleotide primers used in this study

Genes	Primers	Sequence 5'>3'	Amplicon Size, nt
α s1-casein (<i>CSN1S1</i>)	forward	TCC ACT AGG CAC ACA ATA CAC TGA	61
	reverse	GCC AAT GGG ATT AGG GAT GTC	
α s2-casein (<i>CSN1S2</i>)	forward	CTG GTT ATG GTT GGA CTG GAAAA	76
	reverse	AAC ATG CTG GTT GTA TGA AGT AAA GTG	
β -casein (<i>CSN2</i>)	forward	GAA AGC CAG AGC CTG ACT CTC A	63
	reverse	CTG GAC CAG AGC CAG AGG AA	
κ -casein (<i>CSN3</i>)	forward	AGG TGC AAT GAT GAA GAG TTT TTT C	66
	reverse	CCC AAA AAT GGC AGG GTT AA	
α -lactalbumin (<i>LALBA</i>)	forward	TGG TGC AAA GAC GAC CAG AA	64
	reverse	GGA ACT TGT CAC AGG AGA TGT TAC A	
β -lactoglobulin (<i>BLG</i>)	forward	CAT CGT CAC CCA GAC CAT GA	54
	reverse	CAA GTC CCC GCC ACC TTC	
Lactoferrin (<i>LTF</i>)	forward	GAG ACC AAC GGA AGG GTA CCT	59
	reverse	TGA GCC CCT CAT TTG CTT TC	
Osteopontin (<i>OPN</i>)	forward	CCC AGG AGG AGA GCA AGC ATT	66
	reverse	TCT TGG CTG AGT TTG GAA TTT TC	
<i>GlyCAM-1</i>	forward	CTA CCC TTG GAT CAG AAG AGA CTA CA	69
	reverse	TCA GTT TTC CTT CTG TGG TGG AT	
<i>JDP-1</i>	forward	CCC TCC TGT GCT GCC AAC T	91
	reverse	GAT GGA GGA ATG ATT TGG TAC TCA	
Diacylglycerol-O-acyltransferase (<i>DGAT1</i>)	forward	GGC GGT CCC CAA CCA CCT	58
	reverse	GCA GGA GTG GAA GAG CCA GTA	
Stearoyl CoA desaturase (<i>SCD</i>)	forward	TGC TGA CAA CTT ATC TGG ATG C	178
	reverse	AAG GAA TC TGC AAA CAG CTA	
Fatty acid synthase (<i>FASN</i>)	forward	ACA GCC TCT TCC TGT TTG ACG	225
	reverse	CTC TGC ACG ATC AGC TCG AC	
Adipophilin (<i>ADRP</i>)	forward	CCC ACT GTG CTG AGC ACA TT	57
	reverse	GAG TCA GGT TCC GGG CAA T	
FABP-4	forward	TGG TGC TGG AAT GTG TCA TGA	63
	reverse	TGG CTT ATG CTC TCT CGT AAA CTC T	
BMP-7	forward	AAG CAC GAG CTA TAC GTC AGC TT	62
	reverse	TCG GGT GCG ATG ATC CA	
ID-2	forward	GAA GGT GAG CAA GAT GGA AAT CC	191
	reverse	GGA ATT CAG AAG CCT GCA AGG AC	
Elf-5	forward	TCA AGA CTG TCA CAG TCA TAG TCG AA	65
	reverse	CTC GCA CAA ATT CCC ATA GAT G	
Butyrophillin (<i>BTN1A1</i>)	forward	GAT GGC AGT CTT TCC AAA TTC C	88
	reverse	AAA GGG AGC AGA ATC CAG CTT	
Lactadherin (<i>MFGE-8</i>)	forward	TGG ATA ATC AGG GCA AGT TCA A	72
	reverse	GGT CAA TCT GCA GCC ACT CA	
Lactoperoxidase (<i>LPO</i>)	forward	CTC AAC CCT CAC TGG AAT GGA	87
	reverse	GTC CCT AAA GGT GAT GAT CTG TAT GA	
Casein kinase 2 (<i>CNSK-2</i>)	forward	GGA CAT GAC AAT TAT GAT CAG TTG GT	101
	reverse	CGT GGA TCT AAT TCA ATG TTG TAT TTG	
Keratin 14 (<i>KRT-14</i>)	forward	CCC AGC TCA GCA TGA AAG C	57
	reverse	AGC GGC CTT TGG TCT CTT C	
Insulin-like growth factor binding protein 5 (<i>IGFBP5</i>)	forward	CAG AGT AGC CCA CAC GGA TAG A	66
	reverse	ATT CCG AGT TGC CTA CCG G	
Lipin 1 (<i>LPINI</i>)	forward	CCG TTC TAT GCT GCT TTT GGA	64
	reverse	TCG TAC AAG CAA GTG GGA GTG T	
ATP-binding cassette, subfamily G (White), member 2* (<i>ABCG2</i>)	forward	CAT TCC TCG ATA CGG CTA TGC	63
	reverse	TTT GGG ACA AAA CTT CTG CCC	
Chemokine (C-X-C motif) ligand 9* (<i>CXCL9</i>)	forward	GGG CTT GGA AAC CCT CTT AAA	61
	reverse	GCA TAA GAG AGG ATG TCA GGC CA	
24S ribosomal protein (<i>RPS24</i>)	forward	TTT GCC AGC ACC AAC GTT G	66
	reverse	AAG GAA CGC AAG AAC AGA ATG AA	

Each pair of primers amplifies the target cDNA (amplicon sizes ranging between 54 and 225 nucleotides). Primers pairs were designed with Primer Express Software v2.0 (Applied Biosystems) except for 24S ribosomal protein primers, which were manually designed. *Unoptimized qPCR system.

wise, is involved in the establishment and maintenance of endothelial integrity (angiogenesis).

These results show that the goat mammary gland, during pregnancy and lactation, is a very dynamic organ requiring remodeling and high cell turnover. High signal intensities were noted in pregnancy and lactation for genes involved in apoptosis and cellular organization and in regulating transcription and translation. The presence of two casein-encod-

ing genes (*CSN2* and *CSN3*) in this dataset was unexpected, especially in view of their high signal intensity at every stage of pregnancy.

In addition, the protein synthesis function, here mainly represented by genes coding for ribosomal proteins (RPLs), was associated with every stage of pregnancy. Surprisingly, this biological function is not associated with lactation, despite this being a period of intense milk protein biosynthesis.

Table 2. IPA molecular and cellular function of gene sets enriched with the most strongly expressed genes at each developmental stage

Developmental Stage	Probes With Signals Within 10% of the Highest Signal, <i>n</i>	Probes With IPA Annotation (no. of probes without IPA annotation), <i>n</i>	Ingenuity Molecular and Cellular Function
P46	152	78 (49)	protein synthesis cell cycle cell morphology PTM cell death
P70	169	87 (50)	protein synthesis cell death cell cycle cell morphology PTM
P90	175	92 (53)	protein synthesis cell death cell cycle cell movement cell morphology
P110	153	82 (45)	protein synthesis cell death cell cycle cell morphology PTM
L40	130	79 (40)	cell death cell cycle cell morphology PTM cell signaling

Boldface indicates functions that are common to all developmental stages. L, lactation; P, pregnancy; PTM, posttranslational modification. Lists of the most highly expressed genes at each developmental stage are provided in Supplemental data files [highly_expressed_genes_P46](#), [highly_expressed_genes_P70](#), [highly_expressed_genes_P90](#), [highly_expressed_genes_P110](#), [highly_expressed_genes_L40](#).

Comparisons between successive time points. To evaluate differences between two successive developmental stages, four differential analyses were carried out. The first compared 46 and 70 days of pregnancy (P46/P70), the next was aimed at identifying differentially expressed genes (DEG) between 70 and 90 days of pregnancy (P70/P90), the third compared 90 and 110 days of pregnancy (P90/P110), and the last compared 110 days of pregnancy and 40 days of lactation (P110/L40). The number of DEGs (*P* values adjusted using the Benjamini-Hochberg method with a threshold of FDR of 5%) between two successive time points gave the first quantitative indication of differences. There were 2,566 genes differentially expressed between P46 and P70, 448 between P110 and L40, 35 between P70 and P90, and 30 between P90 and P110 (Table 4, also see supplemental material). These figures illustrate the deep functional recasting occurring during pregnancy, especially in early stages and after parturition. This is consistent with the notion that P46, which represents early pregnancy, and L40, which corresponds to established lactation, are extreme developmental stages both very different from the other three stages of pregnancy.

Regarding the P46/P70 comparison, the lowest fold change was 1.4 (210 probes) and the highest 177, corresponding to κ -casein (CSN3), the expression of which increased between P46 and P70. On the other hand, the expression of IGFBP3 (insulin-like growth factor binding protein 3), a protein which

affects cell growth by positively regulating apoptosis and myoblast differentiation and by negatively regulating protein phosphorylation and signal transduction, decreased between P46 and P70. Other genes whose expression decreased between P46 and P70 included COL3A1 (collagen, type III, alpha 1), DCN (decorin), OGN (osteoglycin), PLXNB3 (plexin B3), which participate in organ morphogenesis. Genes whose expression increased between P46 and P70 were mainly involved in immune functions [guanylate binding protein 5 (GBP5), lipopolysaccharide binding protein (LBP), chemokine, C-C motif, ligand 4 (CCL4), immunoglobulin heavy constant alpha 1 (IGHA1) and lactoferrin (LTF)], molecular transport [ubiquitin D (UBD) and retinol binding protein 1 (RBP1)] and cell movement [serpin peptidase inhibitor, clade E (SERPINE2)]. Thus, genes involved in organ morphogenesis showed decreased expression between P46 and P70, whereas the expression of immune response genes increased.

Few genes were differentially expressed between P70 and P90, and only eight genes were upregulated during this period. Twenty-one genes were downregulated, with fold changes ranging between 3.5 and 39, for the genes encoding lactoferrin (LTF) and α_{s2} -casein (CSN1S2), respectively. The same tendency was observed with genes involved in the immune response, including IFI6 (interferon, alpha-inducible protein 6), IFI44L (interferon-induced protein 44-like), and CXCL10 (chemokine, C-X-C motif, ligand 10), as well as BoLA-A, which is a component of the bovine major histocompatibility complex (MHC). CSN3 downregulation between P70 and P90, revealed by the analysis of the most highly expressed genes (Table 3), was confirmed in this comparison.

Again, few genes were differentially expressed between P90 and P110 (*n* = 30); they included genes involved in the regulation of transcription and protein synthesis [mutL homolog 1 (MLH1), synovial apoptosis inhibitor 1 or synoviolin (SYVN1), and heat shock 70 kDa protein 1B (HSPA1B)], which showed decreased expression between P90 and P110. FHOD1 (formin homology 2 domain containing 1) and INHA (inhibin alpha), which participate in cellular organization, showed the same behavior. Some genes upregulated between P90 and P110 are known to be involved in immune responses, including: BoLA-DGA1, BoLA-A, CXCL9 (chemokine, C-X-C motif, ligand 9), GBP5, MBP (myelin basic protein), as well as LTF and TPM3 (tropomyosin 3), which regulates cell motility. During this part of pregnancy, fold changes ranged from 3.2 to 15, respectively for the guanine nucleotide binding protein (GNA13) gene, whose expression decreased, and the major histocompatibility complex (BoLA-DQA1) gene, whose expression increased from P90 to P110, reflecting adjustments rather than deep changes in the gene expression profile.

The transition from late pregnancy to early established lactation (P110/L40) showed once more that the expression of genes involved in immune response (BoLA-A, GBP5), chemoattractant cytokines promoting T cell adhesion to endothelial cells (CXCL9 and CXCL10), and VCAM (vascular cell adhesion molecule 1) which is upregulated by cytokines in endothelial cells, decreased from P110 to L40 (Table 5). In contrast, genes involved in lipid metabolism and secretion [lipoprotein lipase (LPL), butyrophilin (BTN1A1), stearoyl-CoA-desaturase (SCD), and fatty acid binding protein 3 (FABP3)], molecular transport [(NCALD) neurocalcin delta; NADH dehydrogenase, ubiquinone, 1 beta subcomplex, 8, 19

Table 3. 82 probes with high signal intensity at each developmental stage

Encoded Protein	Gene Symbol	Probe Number	GenBank Accession	P46 Signal Intensity	P70 Signal Intensity	P90 Signal Intensity	P110 Signal Intensity	L40 Signal Intensity
Abhydrolase domain containing 6	<i>ABHD6</i>	OLIGO_05640	BM363585	70662	64367	55108	63433	106667
Actin, α :1, skeletal muscle	<i>ACTA1</i>	OLIGO_10461	CR454575	22650	31050	31318	25822	16145
Actin- β	<i>ACTB</i>	OLIGO_10564	AY141970	29377	31095	25831	28848	12223
B-cell CLL/lymphoma 2	<i>BCL2</i>	OLIGO_02195	CN436558	69967	63010	54874	63737	100962
BCL2-associated X protein	<i>BAX</i>	Bt00002710	CK774062	12806	17433	19299	19890	19124
β -2-Microglobulin	<i>B2M</i>	OLIGO_11407	BF440417	10968	23987	15846	22469	15335
		Bt00007118	CK849269	27367	37569	27802	44716	24612
Casein- β	<i>CSN2</i>	OLIGO_12257	S67277	25928	54467	50863	26967	104046
		Bt00007391	CK849815	28103	54410	39221	29941	98833
Casein- κ	<i>CSN3</i>	OLIGO_11992	X00565	19374	56202	18506	21580	103328
Cerebellar degeneration-related protein 1, 34 kDa	<i>CDR1</i>	OLIGO_11327	CR453915	20648	25857	27870	21295	10738
Cytochrome c oxidase subunit 8A (ubiquitous)	<i>COX8A</i>	Bt00000316	CK769747	13706	24849	20057	28151	46645
DAZ-associated protein 1	<i>DAZAP1</i>	OLIGO_11075	EH377586	18023	25615	24865	20848	14649
DEAD (Asp-Glu-Ala-Asp) box polypeptide 46	<i>DDX46</i>	OLIGO_10511	CR453981	28377	29293	27632	24707	12204
EGF-like-domain, multiple 7	<i>EGFL7</i>	OLIGO_12545	EH169691	14265	13166	13925	14400	13288
Eukaryotic translation elongation factor 1 α :1	<i>EEF1A1</i>	OLIGO_10610	CN433968	34200	41181	47041	39983	29081
		Bt00002530	CK773744	59088	57450	54564	57675	51318
Exosome component 8	<i>EXOSC8</i>	Bt00006744	CK848579	18813	17998	20844	19254	18978
Ferritin, heavy polypeptide-like 8	<i>FTHL8</i>	OLIGO_07281	CN434013	43078	46543	45420	36365	26042
Glutathione S-transferase π	<i>GSTP1</i>	OLIGO_10473	EH379175	62282	55992	53868	49250	29459
Glycoprotein M6A	<i>GPM6A</i>	OLIGO_10501	CR551597	21787	30454	31118	26676	14480
		Bt00006995	CK849066	26402	35516	36524	30949	16814
Guanine nucleotide binding protein (G protein), β -polypeptide 2-like 1	<i>GNB2L1</i>	Bt00007200	CK849439	21161	26347	30153	22825	12102
High mobility group AT-hook 1	<i>HMGAI</i>	OLIGO_07163	CR452611	26485	28227	29146	23502	10863
Hypothetical protein LOC339290	<i>LOC339290</i>	Bt00000408	CK769920	15820	17547	18194	14132	11625
Integrator complex subunit 3	<i>INTS3</i>	Bt00000412	CK769926	32148	28522	32901	28292	88903
Keratin 6A	<i>KRT6A</i>	Bt000008172	CK955286	24615	22342	25398	23456	21781
MOB1, Mps one binder kinase activator-like 2C (yeast)	<i>MOBKL2C</i>	Bt00007576	CK943263	13108	15565	16746	17563	14164
Myosin regulatory light chain MRCL3	<i>MRCL3</i>	Bt00007144	CK849324	24658	21134	21884	21536	18470
Opsin 1 (cone pigments), medium-wave-sensitive 2	<i>OPN1MW2</i>	OLIGO_12108	AF280398	12485	12843	14903	13593	16638
Phospholipase D3	<i>PLD3</i>	Bt00003368		36334	36603	33560	34081	50132
Prostaglandin E synthase	<i>PTGES</i>	OLIGO_09243		26519	26191	27397	23697	24878
Ran GTPase activating protein 1	<i>RANGAP1</i>	Bt00005713	CK846479	24926	24811	28180	30320	25624
Ras homolog gene family, member C	<i>RHOC</i>	OLIGO_01134	CR552385	37867	43941	36870	43941	68560
Ribosomal protein L10	<i>RPL10</i>	OLIGO_06837	BF045297	21401	25068	25600	22234	13302
		Bt00007021	CK849109	22023	25798	27725	23311	16193
Ribosomal protein L17-like	<i>HCG</i>	Bt00001141	CK771192	29040	33942	34029	28906	19180
	<i>2004593</i>	OLIGO_06891	CR454801	34954	40961	39388	35710	20690
Ribosomal protein L23	<i>RPL23</i>	OLIGO_10590	CR452075	35538	43368	47155	38707	24053
Ribosomal protein L36a-like	<i>RPL36AL</i>	OLIGO_10917	BM363402	20781	24617	22475	20321	13819
Ribosomal protein L4	<i>RPL4</i>	OLIGO_07375	BF440439	17824	21460	23852	20112	11577
		Bt00007073	CK849184	29534	32697	37322	31176	18124
Ribosomal protein L41	<i>RPL41</i>	OLIGO_10576	AW465014	46969	49141	46586	42458	36860
Ribosomal protein L6	<i>RPL6</i>	OLIGO_10608	BM363457	18222	25688	26952	20950	11027
		Bt00006929	CK848933	26439	31543	35234	26695	15613
Ribosomal protein S10	<i>RPS10</i>	OLIGO_10601	EH165124	11382	18989	19086	14215	12004
Ribosomal protein S11	<i>RPS11</i>	OLIGO_10459	DT842423	27674	35839	35115	31161	19139
Ribosomal protein S2	<i>RPS2</i>	OLIGO_08626	AW466111	15046	17197	22207	16516	11271
Ribosomal protein S23	<i>RPS23</i>	OLIGO_10463	CR454819	27393	34731	34224	27883	16890
		Bt00004836	CK778043	36148	39492	40833	34390	19689
Ribosomal protein S24	<i>RPS24</i>	Bt00006435	CK847945	25467	27000	26670	23064	11748
		OLIGO_10620	CR454824	37205	39034	39562	34866	19127
Ribosomal protein S29	<i>RPS29</i>	OLIGO_10417	CR452232	21494	29688	26417	21878	12710
Signal transducer and activator of transcription 3 (acute-phase response factor)	<i>STAT3</i>	Bt00000335	CK769787	58033	63791	52025	53799	91414
Similar to proline-rich synapse-associated protein 2		OLIGO_09415	CK394152	19122	18117	23367	21015	24599

Continued

Table 3.—Continued

Encoded Protein	Gene Symbol	Probe Number	GenBank Accession	P46 Signal Intensity	P70 Signal Intensity	P90 Signal Intensity	P110 Signal Intensity	L40 Signal Intensity
Solute carrier family 39 (zinc transporter), member 4	<i>SLC39A4</i>	OLIGO_12924	BM429756	13997	13915	14830	14033	13852
SRY (sex-determining region Y)-box 4	<i>SOX4</i>	OLIGO_11229	CN436822	14428	17756	15603	17129	20925
Sterile α -motif and leucine zipper containing kinase AZK	<i>ZAK</i>	OLIGO_10531	CR454290	22383	26670	27027	22517	13504
Survival of motor neuron 1, telomeric	<i>SMN1</i>	Bt00002914	CK774453	40931	39579	43211	39350	44344
TAR (HIV-1) RNA binding protein 2	<i>TARBP2</i>	Bt00002623	CK773899	12008	15372	16636	16040	16239
Transmembrane protein 28	<i>TMEM28</i>	OLIGO_12870	BM253177	11348	13237	14867	14119	17203
Transthyretin (prealbumin, amyloidosis type I)	<i>TTR</i>	OLIGO_08138	BF040485	69094	62820	54502	64261	106021
Transthyretin (prealbumin, amyloidosis type I)	<i>TTR</i>	OLIGO_10391	BM362443	69794	62999	54424	63265	104161
Tumor protein, translationally controlled 1	<i>TPT1</i>	Bt00002885	CK774391	53279	53546	49114	45089	65618
Ubiquitin A-52 residue ribosomal protein fusion product 1	<i>UBA52</i>	OLIGO_06936	CR451887	20428	20667	19977	15421	21285
Ubiquitin fusion degradation 1 like (yeast)	<i>UFD1L</i>	OLIGO_00166	CR550896	14174	13814	14244	14338	15029
Ubiquitin-like protein fubi and ribosomal protein S30		OLIGO_10528	CR454463	19068	19766	19561	18193	10836
Upregulated during skeletal muscle growth 5 homolog (mouse)	<i>USMG5</i>	OLIGO_10361	CR456038	37038	38378	39564	33452	20194
Chromosome 14 open reading frame 133	<i>C14ORF133</i>	OLIGO_10480	CN439899	26068	34910	36416	31874	22422
Chromosome 21 open reading frame 59	<i>C21ORF59</i>	OLIGO_01970	CN435801	11960	12170	13508	12567	18473
NA*	NA	OLIGO_09392	AY563835	13143	12643	13387	13077	14382
NA	NA	Bt00005016		13822	16877	15689	16762	25366
NA	NA	Bt00006423		14407	15038	18180	17149	18549
NA	NA	OLIGO_12452		14874	15260	14934	15171	27193
NA	NA	Bt00000685		15241	15509	15505	16056	15919
NA	NA	OLIGO_00634		15613	11445	17330	13317	14186
NA	NA	Bt00006944		32770	30489	36718	24221	18670
NA	NA	OLIGO_11071	DN845867	33908	39402	29851	28752	26125
NA	NA	Bt00006981	DT895654	34707	41433	42679	39567	65584
NA	NA	Bt00002392		43215	38673	41736	37397	57231
NA	NA	Bt00003641		68770	62161	54954	65248	95884
NA	NA	OLIGO_11122		69876	62228	54291	65667	106850

*NA, probes with no annotation.

kDa (NDUFB8); and nucleoporin 107 kDa (NUP107)], and protein folding [DnaJ homolog, subfamily C, member 12 (JDP-1)] were upregulated. This was also the case for milk protein genes: α_{s1} -, α_{s2} - and β -caseins (CSN1S1, CSN1S2, and CNS2) and α -lactalbumin (LALBA). The CSN3 gene follows the same trend which is significant at a slightly higher FDR threshold (6%). Fold changes ranged from -17.7 (UBD) to 360 (CNS1S1). Finally, while biological functions characterizing late pregnancy are immune response and cell adhesion, lactation is described by lipid metabolism, molecular transport, and milk protein synthesis and protein folding.

Clustering. To better characterize the biological significance of each gene expression profile, we sought clusters of genes that varied significantly at least once in the linear model analysis. In this analysis, the *t*-test applied to the contrasts between estimated parameters allowed us to conclude that 2,330 probes corresponding to 1,696 different genes with IPA annotation varied significantly (*P* values adjusted using the Benjamini-Hochberg method with a threshold of FDR of 15%) at least once in the study. We set the significance threshold at

0.15 to recover a maximum of genes of interest, such as genes coding for milk proteins, which showed significant variations by quantitative PCR. These variations were not significant under the 0.15 threshold, as the fluorescence signal intensity on microarrays saturated at the lactating stage, thus minimizing the differences between stages. The significance threshold of 0.15 was the best compromise between the number of genes for the biological interpretation and the estimated error.

About 73% of these 2,330 probes gave a fluorescence signal <10 times the background signal; 2% were within 10% of the highest signal of the dataset, and 25% had intermediate signals. These genes fell into 19 clusters according to their expression profile (Fig. 2). It must be kept in mind here that the clustering was based on the contrasts of the estimated parameters, in other words on the difference between a given stage and the previous stage ($\theta_i = \mu_{i+1} - \mu_i$). As the distribution was not completely segregated, something that can occur with this clustering method, the lists of genes belonging to clusters with similar profiles were merged for IPA functional analysis into meta-clusters, as follows: *cluster 1* with *clusters 9* and *12* (*meta-*

Table 4. Identification of the IPA biological functions associated with differential analysis between two successive time points

Comparison	Probes Differentially Expressed (different genes, <i>n</i>)	Stages*	Molecular and Cell Function (genes, <i>n</i>)	Physiological System Development and Function (genes, <i>n</i>)
P46/P70	3105 (2566)	P46	gene expression (134)	organism development (143)
		<i>P</i> = 1368	cell growth and proliferation (19)	embryonic development (77)
		<i>G</i> = 991	cell cycle (9)	organ development (103)
		<i>NA</i> = 167	cell movement (41)	nervous system development and function (83)
P70/P90	46 (35)	P70	cell morphology (65)	tissue development (106)
		<i>P</i> = 1737	cell-to-cell signaling and interaction (54)	hematological system development and function (56)
		<i>G</i> = 1167	protein trafficking (12)	immune and lymphatic system development and function (44)
		<i>NA</i> = 241	molecular transport (53)	immune response (67)
P90/P110	33 (30)	P70	cell movement (37)	tissue morphology (7)
		<i>P</i> = 37	cell compromise (8)	nervous system development and function (1)
		<i>G</i> = 21	molecular transport (4)	reproductive system development and function (2)
		<i>NA</i> = 6	cell cycle (4)	tissue development (1)
P110/L40	541 (448)	P90	cell death (5)	immune response (7)
		<i>P</i> = 9	drug metabolism (2)	hematological system development and function (5)
		<i>G</i> = 8	lipid metabolism (2)	reproductive system development and function (2)
		<i>NA</i> = 0	cell cycle (2)	tumor morphology (2)
P90/P110	33 (30)	P90	cell death (5)	organ morphology (2)
		<i>P</i> = 7	cell compromise (4)	skeletal and muscular system development and function (2)
		<i>G</i> = 6	small molecule biochemistry (3)	connective tissue development and function (3)
		<i>NA</i> = 1	DNA replication, recombination and repair (3)	organ morphology (1)
P110/L40	541 (448)	P110	cell-to-cell signaling and interaction (2)	cardiovascular system development and function (2)
		<i>P</i> = 26	cell morphology (1)	hair skin development and function (1)
		<i>G</i> = 17	cell death (1)	embryonic development (1)
		<i>NA</i> = 6	cell assembly and organization (2)	reproductive system development and function (1)
P110/L40	541 (448)	P110	cell signaling (1)	hematological system development and function (10)
		<i>P</i> = 26	cell signaling (7)	immune response (9)
		<i>G</i> = 17	nucleic acid metabolism (4)	skeletal and muscular system development and function (4)
		<i>NA</i> = 6	small molecule biochemistry (7)	immune and lymphatic system development and function (10)
P110/L40	541 (448)	P110	cell movement (6)	cardiovascular system development and function (4)
		<i>P</i> = 223	cell-to-cell signaling and interaction (9)	immune response (52)
		<i>G</i> = 149	cell movement (45)	hematological system development and function (43)
		<i>NA</i> = 28	cell-to-cell signaling and interaction (54)	tissue morphology (34)
P110/L40	541 (448)	L40	cell death (64)	immune and lymphatic system development and function (42)
		<i>P</i> = 318	cell signaling (24)	tissue development (29)
		<i>G</i> = 216	molecular transport (25)	digestive system development and function (2)
		<i>NA</i> = 55	lipid metabolism (26)	immune response (23)
P110/L40	541 (448)	L40	molecular transport (27)	connective tissue development and function (6)
		<i>P</i> = 318	small molecule biochemistry (44)	skeletal and muscular system development and function (13)
		<i>G</i> = 216	cell development (6)	tissue morphology (16)
		<i>NA</i> = 55	cell growth and proliferation (67)	

*P, number of probes; G, number of different genes with IPA annotation; NA, number of probes without IPA annotation. Probes contributing to expression data (fold change, signal intensities) in each comparison between successive time points are provided in supplemental data files Comparison_P46vsP70, Comparison_P70vsP90, Comparison_P90vsP110, Comparison_P110vsL40.

Table 5. Top 25 upregulated and downregulated transcripts in goat mammary tissue at 40 days of lactation compared with 110 days of pregnancy (adjusted *P* value <0.05)

Probe Number*	GenBank Accession	Gene Symbol	Encoded Protein	Log Ratio	Fold Change
<i>Upregulated</i>					
Bt00006833	CK848760	<i>CSN1S1</i>	casein α -s1	8.5	359.8
OLIGO_12085	EE974964	<i>BTN1A1</i>	butyrophilin, subfamily 1, member A1	6.4	84.8
OLIGO_02149	CN436503	<i>NCALD</i>	neurocalcin Δ	6.0	61.9
OLIGO_12034	J05147	<i>LALBA</i>	lactalbumin, α	5.8	55.9
Bt00007030	CK849125	<i>LALBA</i>	lactalbumin, α	5.7	52.2
OLIGO_12366	EH125902	<i>CSN1S2A</i>	casein alpha s2-like A	5.5	46.8
Bt00003265	CK775070	<i>DNAJB11</i>	DnaJ (Hsp40) homolog, subfamily B, member 11	5.3	39.3
OLIGO_10660	BM363051	<i>FABP3</i>	fatty acid binding protein 3	5.3	38.4
Bt00006728	CK848552	<i>FABP3</i>	fatty acid binding protein 3	5.2	36.4
Bt00007007	CK849087	<i>BTN1A1</i>	butyrophilin, subfamily 1, member A1	5.0	33.0
Bt00007059	CK849167	<i>DNAJC12</i>	DnaJ (Hsp40) homolog, subfamily C, member 12	4.9	30.4
Bt00006984	CK849042	<i>NUP107</i>	nucleoporin 107 kDa	4.9	29.6
Bt00002602	CK773866	<i>NDUFB8</i>	NADH dehydrogenase (ubiquinone) 1 β -subcomplex, 8, 19 kDa	4.8	28.8
Bt00007314	CK849661	<i>LPL</i>	lipoprotein lipase	4.8	27.4
Bt00007029	NM_173959	<i>SCD</i>	stearoyl-CoA desaturase (delta-9-desaturase)	4.8	26.9
OLIGO_12092	NM_174528	<i>CSN1S2</i>	casein α -S2	4.6	24.4
Bt00008085	CK953877	<i>CCR3</i>	chemokine (C-C motif) receptor 3	4.5	23.3
Bt00002657	CK773964	<i>C9</i>	complement component 9	4.5	22.2
OLIGO_11838	NM_173933	<i>LPO</i>	lactoperoxidase	4.4	20.7
OLIGO_11285	NM_173959	<i>SCD</i>	stearoyl-CoA desaturase (Δ -9-desaturase)	4.4	20.5
OLIGO_09278	BF041126	<i>DNAJC12</i>	DnaJ (Hsp40) homolog, subfamily C, member 12	4.3	19.7
Bt00006966	CK848999	<i>MED10</i>	mediator complex subunit 10	4.3	19.3
OLIGO_12148	X81699	<i>SLC34A2</i>	solute carrier family 34 (sodium phosphate), member 2	4.2	19.0
Bt00004167	CK776646	<i>PTPN11</i>	protein tyrosine phosphatase, nonreceptor type 11	4.2	18.6
Bt00007394	CK849822	<i>NOP5/NOP58</i>	nucleolar protein NOP5/NOP58	4.2	18.5
<i>Downregulated</i>					
OLIGO_11084	CR452945	<i>COL1A1</i>	collagen, type I, α 1	-2.3	-5.0
OLIGO_06802	CN440096	<i>STMN1</i>	stathmin 1/oncoprotein 18	-2.4	-5.1
Bt00006868	CK848824	<i>CLU</i>	clusterin	-2.4	-5.3
Bt00007372	CK849770	<i>STAT1</i>	signal transducer and activator of transcription 1, 91 kDa	-2.4	-5.3
Bt00007230	CK849494	<i>FCGR2A</i>	Fc fragment of IgG, low affinity IIa, receptor (CD32)	-2.4	-5.5
Bt00007018	CK849105	<i>BoLA-A</i>	major histocompatibility complex, class I, A	-2.5	-5.5
Bt00007214	CK849467	<i>BoLA-A</i>	major histocompatibility complex, class I, A	-2.5	-5.5
Bt00003324	CK775170	<i>PSMB10</i>	proteasome (prosome, macropain) subunit, β -type, 10	-2.5	-5.5
Bt00007310	CK849654	<i>CH13L1</i>	chitinase 3-like 1 (cartilage glycoprotein-39)	-2.5	-5.7
OLIGO_07038	CN435237	<i>OLFML3</i>	olfactomedin-like 3	-2.5	-5.7
OLIGO_08153	CN441870	<i>VCAM1</i>	vascular cell adhesion molecule 1	-2.6	-6.2
OLIGO_10553	CR552676	<i>COL3A1</i>	collagen, type III, α 1	-2.7	-6.3
Bt00006666	CK848411	<i>COL3A1</i>	collagen, type III, α 1	-2.7	-6.5
OLIGO_12360	AV614702	<i>BoLA-A</i>	major histocompatibility complex, class I, A	-2.8	-6.8
OLIGO_11680	BM362485	<i>PSMB9</i>	proteasome (prosome, macropain) subunit, β -type, 9	-2.9	-7.4
OLIGO_10329	EH374936	<i>BoLA-A</i>	major histocompatibility complex, class I, A	-3.0	-7.8
OLIGO_05858	CV798732	<i>GVIN1</i>	GTPase, very large interferon inducible 1	-3.0	-7.9
OLIGO_09615	BM363744	<i>BoLA-A</i>	major histocompatibility complex, class I, A	-3.0	-7.9
OLIGO_05563	BM362452	<i>CXCL9</i>	chemokine (C-X-C motif) ligand 9	-3.0	-8.1
OLIGO_12484	CK955893	<i>CXCL10</i>	chemokine (C-X-C motif) ligand 10	-3.1	-8.8
Bt00007863	CK949281	<i>GBP1</i>	guanylate binding protein 1	-3.2	-9.4
OLIGO_10483	CR452494	<i>COL1A2</i>	collagen, type I, α 2	-3.4	-10.7
Bt00007938	CK950779	<i>UBD</i>	ubiquitin D	-3.7	-12.9
Bt00008202	CK955893	<i>CXCL10</i>	chemokine (C-X-C motif) ligand 10	-3.7	-13.2
OLIGO_05270	BF440277	<i>UBD</i>	ubiquitin D	-4.1	-17.7

*Number Btxxxxxxx corresponds to Bovine Genome Oligoset V1.1 (Operon Biotechnologies); number OLIGO_xxxx corresponds to NCBI GEO reference GPL2853.

cluster A); clusters 5 and 7 (metacluster B); clusters 6 and 8 (metacluster C); cluster 11 with clusters 14 and 16 (metacluster D); and clusters 13 and 15 (metacluster E). Biological functions determined by IPA software associated with each cluster or metacluster are shown in Table 6 (also see supplemental material). No precise descriptions are given for clusters 3 and 10 or for metacluster C, as the biological functions given by IPA were at the limit of significance, and genes belonging

to these groups were not associated with a unique biological function.

Metacluster A (clusters 1, 9, and 12) comprised 218 genes showing an IDID expression profile in the "trajectory" nomenclature (I, increasing; D, decreasing; and F, flat) first proposed by Rudolph et al. (49) to describe the direction of statistically relevant changes between adjacent time points. The most relevant genes in these clusters were CXCL10, CXCR4 (che-

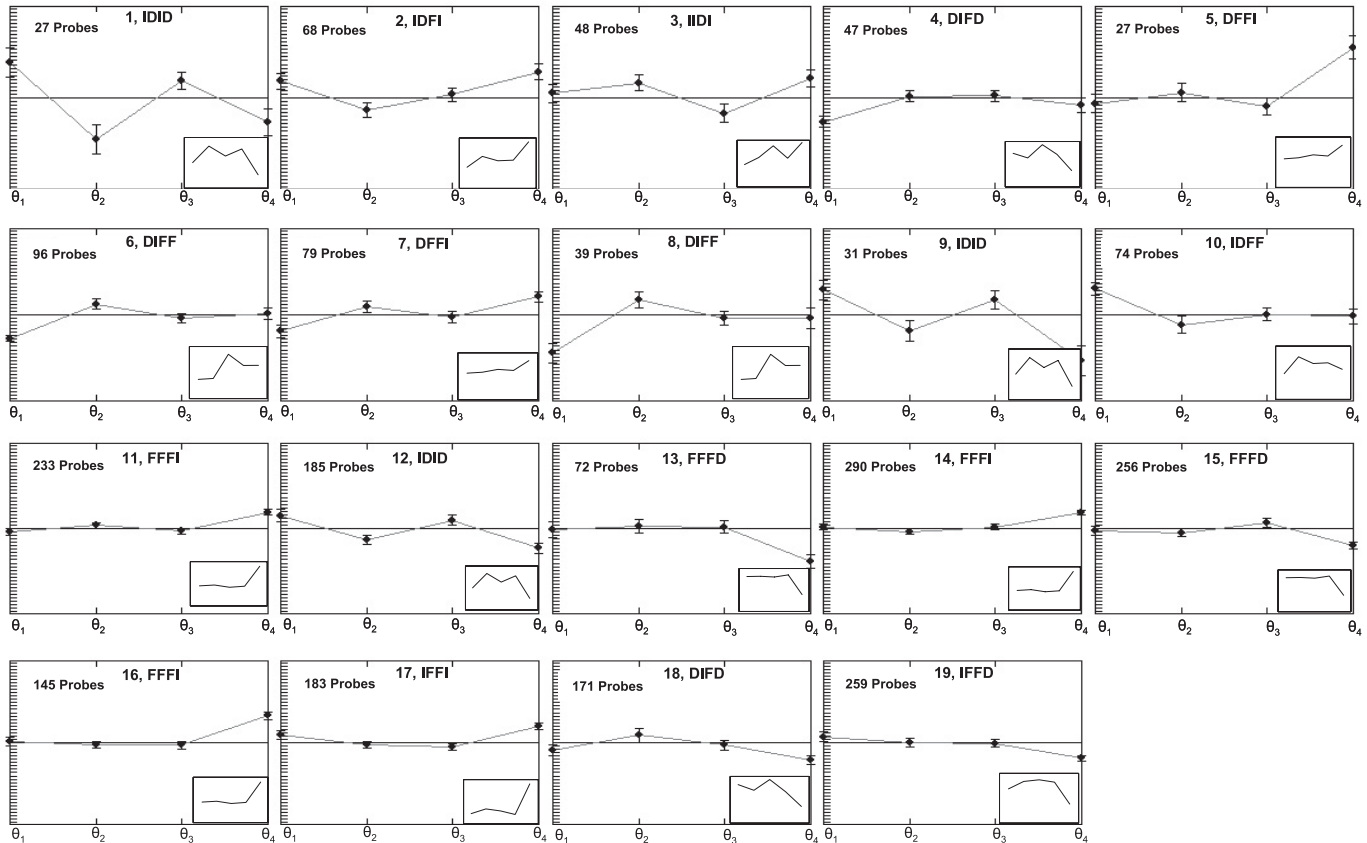


Fig. 2. K-means clustering allocating to 19 clusters the 2,330 probes equivalent to 1,696 genes that varied significantly at least once (in the corner box the gene expression profile drawn from the normalized signal intensity). I, increase; D, decrease; F, flat as proposed by Rudolph et al. (49); θ , difference between one developmental stage and the previous stage. If θ is positive, the gene expression goes up, if θ is negative the gene expression goes down, and if θ is zero the gene expression does not vary.

mokine, C-X-C motif, receptor 4), IL18 (interleukin 18), IL2RG (interleukin 2 receptor, gamma), IRF8 (interferon regulatory factor 8), IFITM3 (interferon-induced transmembrane protein 3), a class of proteins mediating several cellular processes such as homotypic cell adhesion functions of interferons and cellular antiproliferative activities; IFNAR1 (interferon α , β , and ω receptor 1), and BoLA-A and BoLA-DRB1, which encode bovine MHC proteins (class I and II, respectively). These genes were representative of immune and lymphatic system development and function. The IPA canonical pathways associated with the genes present in this metacluster were interferon signaling and antigen presentation pathways.

In *cluster 2* there were 62 genes that showed an IDFI expression profile (Fig. 2). These genes included AP3S1 (adaptor-related protein complex 3, sigma 1 subunit), ERP29 (endoplasmic reticulum protein 29), RAB13 (member RAS oncogene family), SEC22B (vesicle trafficking protein homolog B), SLC36A1 (solute carrier family 36), which encode proteins that participate in molecular transport and protein trafficking.

Cluster 4 contained 43 genes displaying a DFFD expression profile. A representative gene of this cluster is adiponectin (ADIPOQ), which is mainly expressed in and secreted by adipose tissue.

Ninety-four genes belonged to *metacluster B* (*clusters 5 and 7*) displaying a DFFI expression profile. A significant proportion of the genes found in this metacluster ($n = 44$) are

involved in lipid and nucleic acid metabolism, small molecule biochemistry, posttranslational modification, and cell death. One of the canonical pathways associated with these clusters is fatty acid biosynthesis, represented by genes encoding Fatty acid synthase (FASN) and acyl-CoA carboxylase (ACACA).

Clusters 11, 14, and 16 (metacluster D) comprised genes ($n = 551$) with an FFFI expression profile. A significant number of these genes are involved in cell death ($n = 96$) and lipid metabolism and secretion ($n = 47$). Genes participating in lipid metabolism and secretion are exemplified by ABCG2 (ATP-binding cassette, subfamily G, member 2), ACACA, LPL, SDC2 (syndecan 2), FABP2 (fatty acid binding protein 2), LPIN1 (lipin 1), AGPAT1 (1-acylglycerol-3-phosphate O-acyltransferase 1), ACADSB (acyl-Coenzyme A dehydrogenase, short/branched chain), ACSL1 (acyl-CoA synthetase long-chain family member 1), ALDH3B2 (aldehyde dehydrogenase 3 family, member B2), DPAGT1 (dolichyl-phosphate N-acetylglucosaminophosphotransferase 1), and HDLBP (high density lipoprotein binding protein). Genes representative of cell death, such as Bcl-2, which has a well-known antiapoptotic function, and STAT3, shared the same expression pattern.

On the microarray there were three probes corresponding to ACACA. Two of them were directed towards two metaclusters (*B* and *D*), underlining the proximity between these two metaclusters. Surprisingly, the last one did not appear in any of the

Table 6. IPA biological functions associated to each cluster

Cluster	Genes, <i>n</i>	Annotations Recognized by Ingenuity, <i>n</i>	IPA Molecular and Cellular Function (genes, <i>n</i>)	IPA Physiological System Development and Function (genes, <i>n</i>)	IPA Canonical Pathway (ratio)
1, 9, 12 IID	243	218	cell death (49) cell-to-cell signaling and interaction (41) gene expression (13) cellular development (22) DNA replication, recombination, and repair (12) molecular transport (8) protein trafficking (5) amino acid metabolism (3) cell death (1) cell morphology (2) cell morphology (6) amino acid metabolism (2) carbohydrate metabolism (3) cell death (5) cellular function and maintenance (6) gene expression (3) carbohydrate metabolism (2) cell cycle (1) cell death (9) cell morphology (3) lipid metabolism (8) nucleic acid metabolism (4) small molecule biochemistry (13) posttranslational modification (3) cell death (16) cell signaling (14) DNA replication, recombination, and repair (2) nucleic acid metabolism (4) small molecule biochemistry (13) gene expression (20) carbohydrate metabolism (5) small molecule biochemistry (8) cellular development (3) cellular growth and proliferation (3) molecular transport (7)	immune response (50) hematological system development and function (40) immune and lymphatic system development and function (40) tissue morphology (26) embryonic development (11) embryonic development (1) tissue development (1) organ morphology (1) organismal development (1) connective tissue development and function (1) tissue morphology (4) cardiovascular system development and function (3) digestive system development and function (1) endocrine system development and function (3) organ morphology (6) cardiovascular system development and function (2) endocrine system development and function (2) hair and skin development and function (1) hematological system development and function (2) immune and lymphatic system development and function (2) hematological system development and function (3) cardiovascular system development and function (4) digestive system development and function (4) embryonic development (3) endocrine system development and function (3) organismal development (15) behavior (8) cardiovascular system development and function (9) nervous system development and function (14) tissue morphology (7) embryonic development (5) tissue morphology (6) tumor morphology (3) cardiovascular system development and function (3) organ development (4)	interferon signaling (9/29) protein ubiquitination pathway (14/203) antigen presentation pathway (6/39) hepatic fibrosis/ hepatic stellate cell activation (6/131) D-glutamine and D-glutamate metabolism (2/27) cell cycle: G1/S checkpoint regulation (2/60) glutathione metabolism (2/104) taurine and hypotaurine metabolism (1/47) mitochondrial dysfunction (2/165) arachidonic acid metabolism (2/211) fatty acid biosynthesis (1/49) G protein-coupled receptor signaling (2/199) keratan sulfate biosynthesis (1/49) urea cycle and metabolism of amino groups (1/80) N-glycan biosynthesis (1/87) glycosphingolipid biosynthesis - lactoseries (1/28) O-glycan biosynthesis (1/43) glycosphingolipid biosynthesis - globoseries (1/41) glycosphingolipid biosynthesis - ganglioseries (1/58) keratan sulfate biosynthesis (1/49) fatty acid biosynthesis (2/49) LXR/RXR activation (3/81) aryl hydrocarbon receptor signaling (3/152) pyruvate metabolism (2/145) TGF- β signaling (2/83) VDR/RXR activation (3/80) ERK/MAPK signaling (4/226) inositol phosphate metabolism (3/173) Wnt/ β -catenin signaling (3/165) cAMP-mediated signaling (3/159) oxidative phosphorylation (7/158) ubiquitome biosynthesis (4/105) mitochondrial dysfunction (5/165) valine, leucine, and isoleucine degradation (3/107) citrate cycle (2/59)
2 IDFI	68	62			
3 IIDI	48	40			
4	47	43			
DIFD					
5, 7	106	94			
DIFF					
6, 8 DIFF	135	114			
10 IDFF	74	63			

Continued

Table 6.—Continued

Cluster	Genes, <i>n</i>	Annotations Recognized by Ingenuity, <i>n</i>	IPA Molecular and Cellular function (genes, <i>n</i>)	IPA Physiological System Development and Function (genes, <i>n</i>)	IPA Canonical Pathway (ratio)
11, 14, 16	668	551	cell death (96) cellular growth and proliferation (3) cardiovascular system development and function (3) cellular response to therapeutics (4) cellular function and maintenance (22) cellular movement (57) lipid metabolism (47) cellular development (44) cell cycle (34) cell morphology (43) gene expression (38) cellular growth and proliferation (70) carbohydrate metabolism (10)	renal and urological system development and function (9) valine, leucine, and isoleucine degradation (3/107) cardiovascular system development and function (25) tissue development (30) connective tissue development and function (33) hair and skin development and function (14) immune response (34) hematological system development and function (34) immune and lymphatic system development and function (33) tissue morphology (30) connective tissue development and function (6) skeletal and muscular system development and function (6) hematological system development and function (11) immune response (10) cardiovascular system development and function (7) connective tissue development and function (13) skeletal and muscular system development and function (7) hematological system development and function (10) immune response (6) immune and lymphatic system development and function (10) cardiovascular system development and function (10) immune response (6) immune and lymphatic system development and function (13) cardiovascular system development and function (3) immune and lymphatic system development and function (13) tissue development (6) digestive system development and function (3) skeletal and muscular system development and function (9)	LXR/RXR activation (9/81) acute phase response signaling (12/172) Hepatic fibrosis/hepatic stellate cell activation (10/131) LPS/IL-1-mediated inhibition of RXR function (13/195) EGF signaling (6/47) antigen presentation pathway (4/39) IL-4 Signaling (5/68) T cell receptor signaling (6/102) B cell receptor signaling (7/148) Glucocorticoid receptor signaling (9/265) N-glycan biosynthesis (3/87) integrin signaling (5/192) calcium signaling (4/204) arginine and proline metabolism (3/178) urea cycle and metabolism of amino groups (2/) p53 signaling (5/87) VDR/RXR activation (3/80) Wnt/ β -catenin signaling (4/165) hepatic fibrosis/hepatic stellate cell activation (3/131) Huntington's disease signaling (4/232) protein ubiquitination pathway (9/203) estrogen receptor signaling (5/118) selenoamino acid metabolism (3/69) methionine metabolism (3/76) synthesis and degradation of ketone bodies (2/19)
FFFI					
13, 15 FFFD	328	287	cell morphology (43) gene expression (38) cellular growth and proliferation (70) carbohydrate metabolism (10) nucleic acid metabolism (7) small molecule biochemistry (21) cellular assembly and organization (9) amino acid metabolism (8) RNA posttranscriptional modification (8) gene expression (13) cellular development (12) cell morphology (14) cellular growth and proliferation (36) cellular growth and proliferation (36) protein synthesis (15) cell-to-cell signaling and interaction (8) carbohydrate metabolism (5) cellular development (13)	immune and lymphatic system development and function (33) hair and skin development and function (14) immune response (34) hematological system development and function (34) immune and lymphatic system development and function (33) tissue morphology (30) connective tissue development and function (6) skeletal and muscular system development and function (6) hematological system development and function (11) immune response (10) cardiovascular system development and function (7) connective tissue development and function (13) skeletal and muscular system development and function (7) hematological system development and function (10) immune response (6) immune and lymphatic system development and function (10) cardiovascular system development and function (10) immune response (6) immune and lymphatic system development and function (13) cardiovascular system development and function (3) immune and lymphatic system development and function (13) tissue development (6) digestive system development and function (3) skeletal and muscular system development and function (9)	
17	183	153			
IFFI					
18	171	158			
DIFD					
19	259	229			
IFFD					

Probes contributing to expression data (signal intensities) in each comparison between successive time points are provided in supplemental data files Cluster_2, Cluster_3, Cluster_4, Cluster_10, Cluster_17, Cluster_18, Cluster_19, Metacluster_A, Metacluster_B, Metacluster_C, Metacluster_D, Metacluster_E.

19 clusters. This was due to weak variability, very close to the threshold of significance.

Metacluster E (clusters 13 and 15) comprised 287 genes downregulated in lactation (FFFD). This metacluster is associated with the following biological functions: immune response and immune and lymphatic system development, which are allocated, at the molecular and cell level, to cell development, cell cycle, cell growth, and proliferation. Canonical pathways associated with this profile are antigen presentation pathways, IL-4 signaling, and T-cell and B-cell receptor signaling. Some representative genes are CD74, BoLA-A, BoLA-DMB, and BoLA-DRB1, which belong to the bovine MHC, IL2RG, and IL4R (interleukin 4 receptor), which are interleukin receptors, and NFATC2 (nuclear factor of activated T-cells, cytoplasmic, calcineurin-dependent 2), which is a positive regulator of transcription.

Cluster 17 contained 153 genes with an IFFI expression pattern. These genes included UGP2 (UDP-glucose pyrophosphorylase) and B4GALT1 (UDP-Gal:betaGlcNAc beta 1,4-galactosyltransferase, polypeptide 1), which contribute to carbohydrate metabolism, including lactose synthesis. This cluster also contained genes encoding milk proteins such as α_{s1} -casein (CSN1S1) and β -casein (CSN2), confirming that many of the genes involved in milk synthesis and secretion are transcribed before the onset of lactation.

Cluster 18 contained 158 genes with a DIFD expression profile and mainly involved in RNA posttranscriptional modification and gene expression. This cluster included genes coding for splicing proteins such as SF3B3 (splicing factor 3b, subunit 3), SFRS4 (splicing factor, arginine/serine-rich 4), SFRS7 (splicing factor, arginine/serine-rich 7), SFRS12 (splicing factor, arginine/serine-rich 12), SFRS (splicing factor, arginine/serine-rich), and also DNA replication or transcription factors such as HMGB1, MED1 (mediator complex subunit 1), SSRP1 (structure specific recognition protein 1), and WT1 (Wilms tumor 1).

Finally, *cluster 19* grouped together 229 genes with an IFFD expression profile. These genes were representative of cell growth and proliferation and protein synthesis. Genes in this cluster contribute to several biological functions. One encodes the local factor C/EBP β , which is involved in the cell fate decision leading to progesterone receptor expression and then affects cell proliferation through a paracrine mechanism (22).

Validation of microarray results by qPCR. Some results of the microarray analysis were validated by qPCR applied to the same mammary tissue samples. In addition, as some specific genes that were expected to be differentially expressed (involved in milk protein biosynthesis, milk fat globule biogenesis, or mammary tissue development) were not correctly analyzed by the microarray approach (signal saturation for several probes), their expression profiles were specifically analyzed by qPCR and then compared with the microarray results. A set of 19 PCR systems was designed to analyze the expression of genes involved in biosynthesis and secretion of lipids (DGAT1, SCD, FASN, ADRP, FABP4, MFGE8, BTN1A1) and milk proteins (CSN1S1, CSN1S2, CSN2, CSN3, LALBA, LTF, LPO), and mammary tissue development (BMP-7, ID-2, OPN), as well as ubiquitous genes (JDP-1, CSNK2A2). In addition, four genes relevant to mammary function but absent from the probe repertoire on microarrays (KRT14, GLYCAM1, BLG, Elf5) and four genes representative of two main clustering

expression profiles (CXCL9, ABCG2, IGFBP5, LPIN1) were also analyzed.

The microarray and qPCR expression profiles were compatible for most of the genes investigated, with a global correlation coefficient close to 0.82 (Figs. 3 and 4). Genes with discrepant results between qPCR and the microarray approach included DGAT1, CSN1S2, CSN2 and CSN3 (Fig. 3). DGAT1 (Fig. 3A) gave weak signal intensity at every stage. As the DGAT1 mRNA sequence is incomplete for *Capra hircus* and *Ovis aries*, we compared the nucleotide sequence of the DGAT1 oligonucleotide probe printed on the microarray with the DGAT1 mRNA sequence of *Bos taurus* (NCBI: NM_174693), *Homo sapiens* (NCBI: NM_012079), *Mus musculus* (NCBI: NM_010046), *Sus scrofa* (NCBI: AY093657), and *Bubalus bubalis* (NCBI: DQ886485). The number of mismatches was respectively 0, 30, 30, 19, and 4. This region seems highly variable across species, suggesting the potential occurrence of mismatches between the probe spotted on the microarray (*B. taurus* sequence) and the *C. hircus* mRNA sequence, possibly explaining the weak signal intensity and the absence of differences between developmental stages in the microarray method. For most of the genes encoding major milk proteins (Fig. 3B), changes between stages, for instance between L40 and P70, were higher with qPCR than with microarray analysis. This is probably due to saturation of the fluorescence signal on the microarrays, leading to an underestimation of the differences.

Regarding lipid biosynthesis and secretion, two types of gene expression profile were observed (Fig. 3A). The first corresponds to genes generally strongly expressed during lactation (BTN1A1, SCD, MFGE-8) and the second to genes more or less expressed at every stage of pregnancy (FASN, ADRP, FABP4) and upregulated during lactation. Milk protein genes could be divided into three classes according to their expression profiles (Fig. 3B), including: 1) genes that are expressed at mid-pregnancy and that are highly expressed during lactation (CSN2, CSN1S2, CSN3 and LALBA); 2) genes that are highly expressed only during lactation (CSN1S1 and LPO); and 3) genes that are highly expressed at midpregnancy and weakly expressed during lactation (OPN and LTF). Genes known for their involvement in mammary tissue development (BMP-7 and ID-2) were expressed at every developmental stage (Fig. 3C), and CSNK2A2 displayed the same pattern of expression.

To validate expression profiles obtained by clustering, key genes belonging to trajectory *metaclusters D* and *A* were selected and analyzed. LPIN1, ABCG2 and IGFBP5 (*metacluster D*) showed, as expected, drastic upregulation during lactation. Likewise, CXCL9 which follows the same profile as genes in *metacluster A* (not included in this metacluster because of borderline statistical significance, but functionally interesting) was confirmed as being upregulated at P70 and P110 (Fig. 4).

Finally, among the key genes of interest absent from the microarray (Fig. 5), JDP-1, BLG, and GLYCAM1 showed high expression during lactation, whereas Elf5 also displayed significant expression at P70. In contrast, KRT14 was equally expressed at every developmental stage, suggesting that myo-epithelial cells are present very early in pregnancy and that their numbers change little during pregnancy and the transition to lactation. This is not really surprising, as these cells are

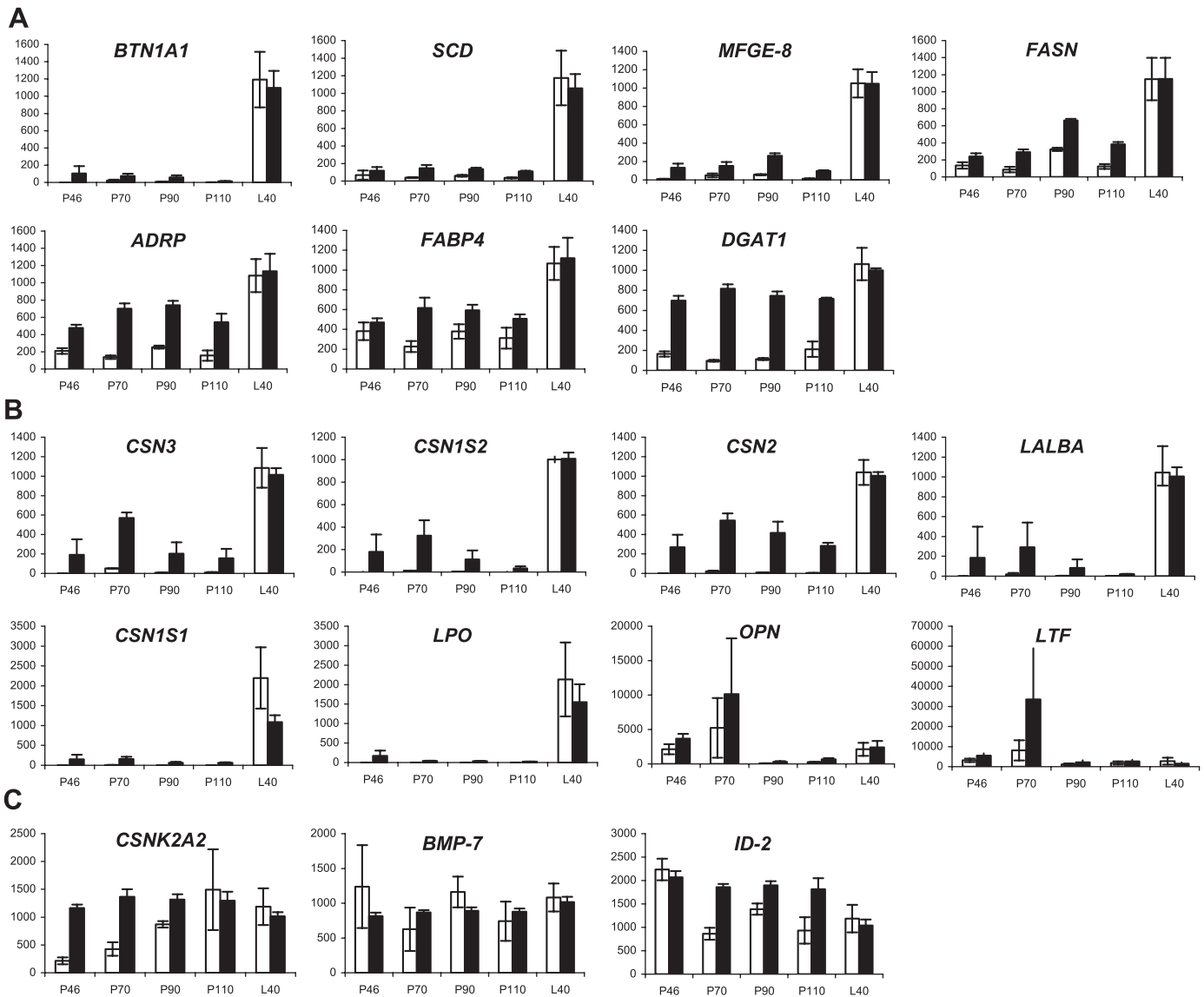


Fig. 3. Gene expression profiles obtained by qPCR and microarray analysis. *A*: lipid biosynthesis genes; *B*: milk protein genes; *C*: mammary setting and ubiquitous genes. *BTN1A1*, butyrophillin; *SCD*, stearyl CoA desaturase; *MFGE-8*, milk fat globule-EGF factor 8; *FASN*, fatty acid synthase; *ADRP*, adipophillin; *FABP4*, fatty acid binding protein 4; *DGAT1*, diacylglycerol acyltransferase 1; *CSN3*, casein κ ; *CSN1S2*, casein α_{S2} ; *CSN2*, casein β ; *LALBA*, α -lactalbumin; *CSN1S1*, casein α_{S1} ; *LPO*, lactoperoxidase; *OPN*, oestropontin; *LTF*, lactoferrin; *CSNK2A2*, casein kinase 2; *BMP-7*, bone morphogenetic protein 7; *ID-2*, inhibitor of DNA binding 2. White (qPCR) and black (microarray) bars represent the relative abundance of target transcripts at the different stages of pregnancy, determined assuming the expression of individual lactation was 1,000.

known to aid in milk ejection and also to regulate ductal morphogenesis in mice during pregnancy (40).

Morphological differentiation of the goat mammary gland during pregnancy and lactation. During pregnancy the mammary gland undergoes profound structural reorganization, with the formation of secondary branches and extensive lobulo-alveolar development, primarily driven by progesterone. This phase of differentiation results in a sharp increase in the number of luminal epithelial cells (MEC). As previously reported (24), in ruminants, the ducts and lobular units are separated from adipocytes by multiple layers of fibroblastic connective tissue. Histological changes in goat mammary gland morphology during pregnancy and lactation are shown in Fig. 6. Unfortunately, owing to the small amount of mammary tissue available at P46, we could not perform any morpholog-

ical studies at this stage, all the material sampled being used for gene expression profiling. At midpregnancy (P70), the ratio between the area occupied by MEC (pink-brown area in Fig. 6A) and stromal tissue was $\sim 30\%$. At P90 (Fig. 6C), the area of LAS increased in the stromal parenchyma. Later in pregnancy (P110, Fig. 6E), inter- and intralobular stromal tissues regressed to an average of $<10\%$ during lactation (L40, Fig. 6G), even though development was sometimes heterogeneous across different sections. While it is quite easy to identify LAS and alveolar epithelial cells, it is difficult to distinguish other cell types in this abundant connective tissue without using specific immunohistological approaches.

As shown in Fig. 6B, at higher magnification the alveoli in midpregnancy (P70) are completely or partially filled with MEC. At P90 the alveolar lumen is more open and MEC are

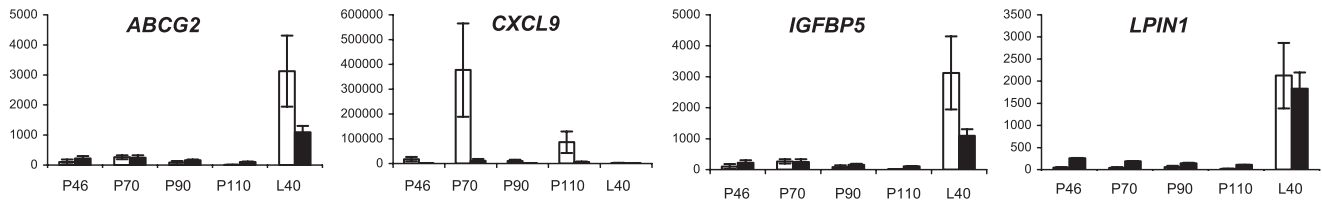


Fig. 4. Gene expression profiles obtained by qPCR and microarray analysis of genes representative of expression profiles corresponding to *metaclusters A* and *D*. ABCG2, ATP-binding cassette subfamily G (white), member 2; CXCL9, chemokine (C-X-C motif) ligand 9; IGFBP5, insulin-like growth factor binding protein 5; LPIN1, lipin 1. White (qPCR) and black (microarray) bars represent the relative abundance (determined assuming the expression of individual lactation was 1,000) of target transcripts at the different stages of pregnancy.

organized in one or two layers (Fig. 6D). At P110, MEC organization strongly resembles a monolayer (Fig. 6F) and, within the expanding luminal space, the presence of secretory material very similar to milk, with lipid droplets (white spots), can be observed, pressing the epithelial cells against the alveolar wall. During lactation (Fig. 6H), we distinguished MEC monolayers within alveoli. The lumen was very thin and empty, as the goats were milked before slaughter.

DISCUSSION

This is the first global gene expression study designed to follow changes in ruminant mammary gland ontogeny during pregnancy. We chose to study goats, as they are smaller and cheaper than cattle. As pregnancy lasts ~150 days in goats, P46 represents the end of the first third of pregnancy and P70 the end of the first half.

Three findings with respect to goat mammary gland terminal differentiation are particularly noteworthy. First, the first half of pregnancy was characterized by downregulation of genes usually expressed in adipocytes, whereas genes whose expression is usually considered representative of a differentiated mammary epithelium, such as genes coding for immune function and milk proteins, were already expressed. Second, a switch occurred between late pregnancy (P110) and established lactation characterized by downregulation of genes associated with immune functions, whereas genes coding for lipids and lactose biosynthesis and secretion were strongly upregulated.

The third important result is the upregulation of genes encoding proteins involved in both innate and specific immunity at midpregnancy (P70) and at the beginning of the last third of pregnancy (P110).

Changes in cell composition during the first half of pregnancy. Histological changes occurring in the goat mammary gland during the first half of pregnancy (Fig. 6) were consistent with gene expression data (see thereafter) and confirm that the functional differentiation process of goat mammary gland is similar to that previously reported for mice (4). Between P46 and P70, a fall was noted in the ratio of interlobular stromal tissue (mainly composed of adipocytes and fibroblasts in ruminants) to secretory tissue (primarily composed of epithelial and myoepithelial cells). This decrease follows a reduction in the expression of adipocyte markers such as adiponectin (26) (belonging to *cluster 4*) and PPAR γ (32), FGF-10 (43) and fibroblast markers such as S100A4 and vimentin (VIM).

In addition, genes involved in mice lobulo-alveolar development and differentiation (4), such as VEGF and sterol regulatory element binding transcription factor 1 (SREBF1), were downregulated, while Elf5 and cyclin D1 (CCND1) were upregulated between P46 and P70, suggesting that differentiation of goat mammary tissue follows the same pattern as that of mice mammary tissue. ID2, which is required for lobulo-alveolar development (36), is significantly expressed during pregnancy in goat mammary tissue. In mice, the switch be-

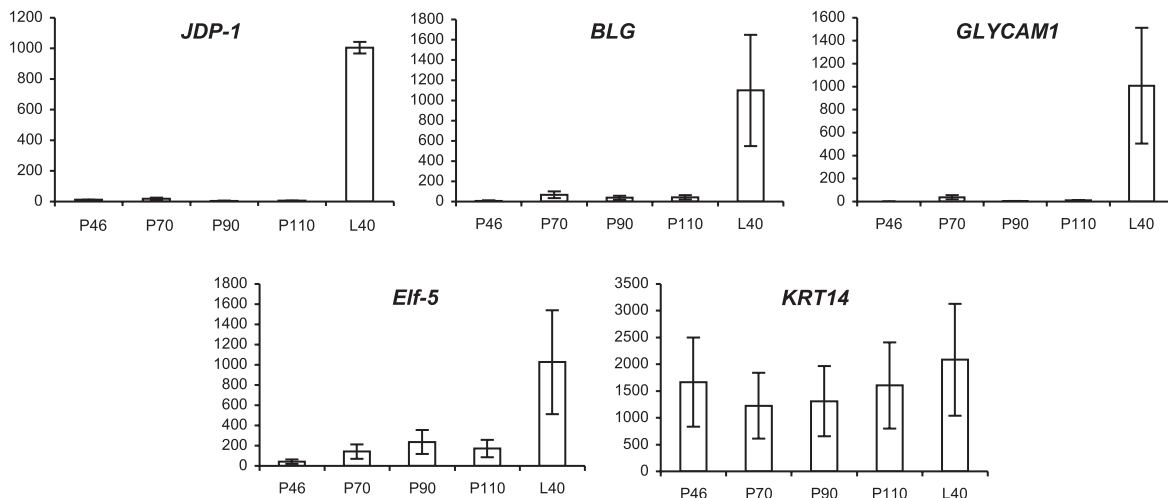


Fig. 5. Gene expression profiles obtained by qPCR of genes relevant to mammary function and absent from the repertoire printed on microarrays. BLG, β -lactoglobulin; GLYCAM1, glycosylation dependent cell adhesion molecule 1; Elf-5, E74-like factor 5; KRT14, keratin 14. White bars represent the relative abundance of target transcripts at the different stages of pregnancy, determined assuming the expression of individual lactation was 1,000.

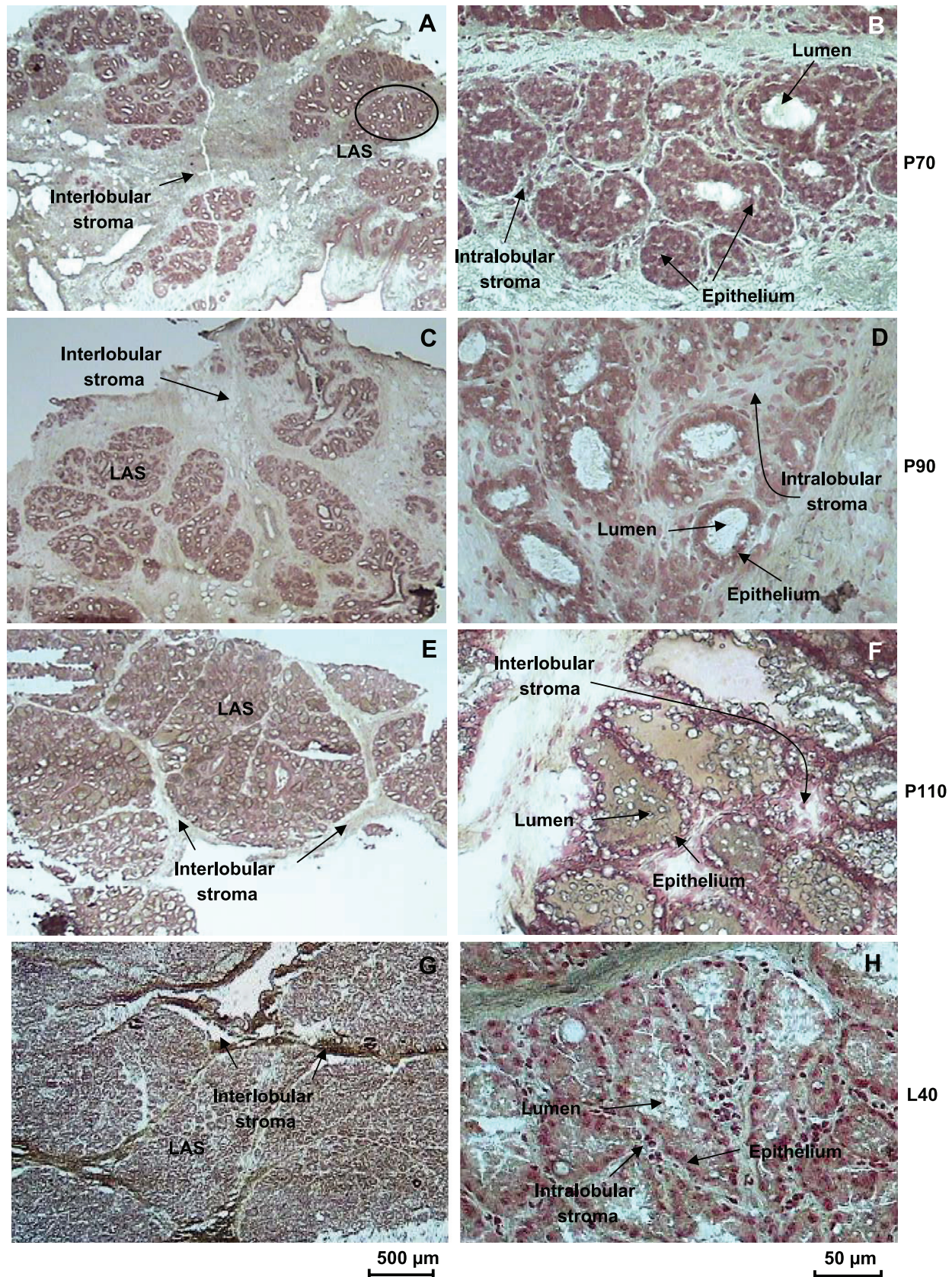


Fig. 6. Histological sections of goat mammary tissue during pregnancy and lactation. Mammary glands were taken from goats on *day 70* (P70, A and B), *day 90* (P90, C and D), and *day 110* (P110, E and F) of pregnancy and on *day 40* (L40, G and H) of lactation, then frozen in liquid nitrogen, sectioned, and stained with hematoxylin. On the *left* micrographs (A, C, E, and G) the scale bars represent 500 μm , whereas those on the *right* (B, D, F, and H) represent 50 μm . LAS, lobuloalveolar structure.

tween the first third and midpregnancy is characterized by lobulo-alveolar development accompanied by cell proliferation (4, 23, 44, 47).

Therefore, our results suggest that, between P46 and P70, the goat mammary gland changes from a stromal tissue composed of adipocytes and fibroblasts to an organized lobulo-alveolar tissue with an epithelium internally coating alveoli in which milk will be synthesized and secreted after parturition. This is compatible with histological observations (Fig. 6) and morphological findings obtained in 1979 by Swanson and Poffenbarger (59), who found that bovine mammary tissue already has alveolar structures at midpregnancy (5 mo in their study). This reminds us that the gene expression data derived from this comparison must be interpreted with care, as, during the first half of pregnancy, the mammary gland, which is a complex organ composed of different cell types, undergoes marked structural modifications and profound changes in the proportion of the different cell types. By adjusting gene expression values to changes in the size of cell type-specific compartments, Wang et al. (62) show that it is possible to increase both the sensitivity and the specificity of differential gene expression analyses and to assess variations in gene expression due to intrinsic intracellular regulation rather than shifts in the relative cell type abundance (62). However, this “deconvolution strategy” requires either precise characterization of the two major cellular compartments (epithelial and stromal, themselves composed of different cell types) or the use of homogeneous cell populations to derive specific panels of transcripts. Such an approach could not be applied to the goat model.

Epithelial differentiation and activation of secretion. The array data revealed that genes encoding κ -casein and, to a lesser extent, α_{s2} - and β -caseins, α -lactalbumin, and β -lactoglobulin are already expressed at midpregnancy in goat mammary tissue. Moreover, Elf5, a member of the Ets transcription factor family (epithelium-specific subclass) that regulates a number of epithelium-specific genes found in tissues containing glandular epithelium, was also expressed at midpregnancy. In mouse mammary tissue, milk protein synthesis is regulated by two transcription factors: Stat5 and Elf5 (4). The presence of Elf5 and milk protein transcripts in goat mammary tissue at midpregnancy complies with the theory developed for mouse mammary tissue according to which, at midpregnancy, there are sufficient differentiated MEC to express markers of milk synthesis (47). Milk protein genes are weakly expressed in goat mammary tissue during pregnancy, as also previously shown in mice, using an immunohistochemical approach (27). Semi-quantitative Western blot analysis of α_{s1} - and β -caseins in epithelial cell fractions from mouse mammary gland showed that intraepithelial caseins are present at trace levels during the initial stages of pregnancy (between *days 0* and *4*), decline to even lower levels during midpregnancy (*days 6* to *8*), and then rise to high levels during the last third of pregnancy (*day 14*). At the messenger level, based on our qPCR data, we noted a trend toward a slight increase in the expression of casein-encoding genes at midpregnancy, especially CSN3 (κ -casein). However, casein synthesis can be substantially regulated at the level of translation (15). In both goat and mice, the expression of milk protein genes remains very limited during pregnancy compared with the burst occurring at the onset of lactation (>1,000-fold, based on qPCR results), when the mammary

gland is completely differentiated and produces huge amounts of milk. The fold change obtained with the microarray technology was more limited (359-fold), with α_{s1} -casein transcripts between P110 and L40. This result is not in complete agreement with the microarray results obtained by Finucane et al. (20) for bovine mammary gland at the onset of lactation, using the Affymetrix Genechip Bovine Genome Arrays (23,000 gene probes). These authors report that none of the milk protein genes showed significant changes in expression from late pregnancy (5 days before parturition) to early lactation (10 days after parturition). This discrepancy is probably due, at least in part, to the larger interval between the last stage of pregnancy taken into account in our study (P110, 40 days before parturition), compared with 5 days in the Finucane study. However, in mice, the expression of milk protein genes increases gradually during pregnancy, especially in the last part of pregnancy, and there is no sharp increase at secretory activation (parturition), except for δ -casein, α -lactalbumin, and the major milk mucin MUC1 (4).

In the pregnant goat mammary gland, milk protein genes were not the only highly expressed genes. Genes involved in lipid biosynthesis and secretion were also significantly expressed. Indeed, microarray analysis showed that adipophilin (ADRP), acyl CoA:diacylglycerol transferase 1 (DGAT1), fatty acid binding protein 4 (FABP4), and fatty acid synthase (FASN) are expressed throughout pregnancy. This result, which was confirmed and validated by qPCR, is not really surprising, as fatty acid synthase activity has been already measured in the mammary gland of pregnant cows (34) and rabbits (33) and as ADRP mRNA is also found in pregnant mouse mammary gland (4). This is consistent with the fact that, during pregnancy, cell proliferation requires the synthesis of many membranous lipids composed of long-chain fatty acids (as reviewed by Ref. 34) and also with the presence of a significant proportion of adipocytes in the early stages of pregnancy. Thus, the lipid synthesis activity observed in goat mammary gland during pregnancy would not be dedicated to milk synthesis and secretion but rather to the cell proliferation associated with mammary gland development, which requires membrane biosynthesis. The expression of DGAT1 during pregnancy contributes to epithelial proliferation and alveolar development of mammary tissue. This finding is in agreement with results showing that mice lacking the triglyceride synthesis enzyme (DGAT1) have impaired mammary gland development characterized by decreased epithelial proliferation and alveolar development and reduced expression of markers of functional differentiation (13).

Nevertheless, genes involved in milk lipid biosynthesis such as LPL, the long chain acylCoA synthetase homolog 1 (ACSL1) and lipin1 (LPIN1), as well as in lactose synthesis, such as UGP2 and B4GALT1 (*metacluster D* and *cluster 17*), were sharply upregulated in the goat mammary gland after parturition (Table 5). Likewise, Akt1, a serine/threonine protein kinase with a key role in the regulation of glucose transport and lipid metabolism (4, 53) was significantly upregulated between P110 and L40 (*metacluster D*). Butyrophilin (BTN1A1), which is thought to be an activator of milk secretion (41), followed the same pattern (Table 5 and Fig. 3A). SREBF1, which is a central node in the milk lipid metabolism network and controls the transcription of most of the genes that regulate milk fat synthesis in mice (49) and cattle (9), is also a

critical regulator of transcription in goat, as many genes regulated by this factor (ACACA, FASN, LPL, ACSL1, and INSIG1) and showing the same expression pattern (FFFFI), were identified in our study.

In addition, the gene encoding α_{s1} -casein (CSN1S1), the expression profile of which was somewhat different from that of other casein transcripts, as confirmed by qPCR (Fig. 3, *pattern B*), seems to be significantly expressed only during lactation. This observation is consistent with the notion that α_{s1} -casein could be necessary for casein secretion in goat mammary tissue (14).

At the transition from pregnancy to lactation, our study and that of Finucane et al. (20) identified only three common genes among the top 50 differentially expressed genes, namely those encoding lactoperoxidase (LPO), lipoprotein lipase (LPL), and lipin 1 (LPIN1). As Finucane et al. compared the time points 5 days before and 10 days after parturition, while we compared time points 40 days before and after parturition, the expression of LPO, LPL and LPIN1 would appear to be sharply increased (~20-fold for LPO and LPL) after parturition. On the other hand, transcript levels of genes (CSN1S1, CSN1S2, LALBA, BTN1A1, FABP3, SCD) that were upregulated only during lactation in our study are likely to have increased gradually until parturition, based on our qPCR results and on previous studies of mouse mammary tissue (4, 49, 50).

General biological functions associated with lactating mammary gland validate the conclusion, supported by our study, that the lactating stage is characterized by molecular transport, cell movement and protein trafficking. Thus, activation of secretion seems to occur only after parturition in the mammary gland of ruminants, including cows (20), and also in mice (4).

Expression of genes of immunity during pregnancy marks tissue remodeling and differentiation. We observed the expression of immune cell signaling genes in the mammary gland of pregnant nulliparous goats. Most of the genes with an IDID expression profile (increased expression at midpregnancy and at 110 days of pregnancy) code for proteins involved in innate and specific immunity.

Genes of innate immunity code for proteins of the complement system (C1QB, CD2, CD3E, CD69, CD84, CD96), interferons, interferon regulatory factors and receptors (IRF1, IRF2, IRF8, IFNAR1), interleukins and interleukin receptors (IL18, IL2RG), chemokines and chemokine receptors (CCL5, CXCL10, CXCR4), and receptors of natural killer cells (KLRK1) or macrophages (MSR1). We also noted the expression of genes coding for receptors involved in the innate response activation to viral infection (TLR3), or protein effectors of innate immunity such as lactoferrin and lysosomal proteases (cathepsins C and S). Genes of specific immunity were mainly genes coding for immunoglobulin receptors with high affinity for the Fc portion of IgG (FCGR3A) or IgE (FCER1G), or for bovine MHC (BoLA-A, BoLA-DMB, BoLA-DRB1). There were also effectors of the immune response, with the expression of genes encoding proteins of the multicatalytic proteinase complex immunoproteasome (PSMB8, PSME1, PSME2). Interaction networks between these genes that share the same expression profile (*metacluster A*), using IPA for enrichment, in gene sets related to molecular and cell functions (Fig. 7), suggest a central role for IRF1 and IRF2 and for signal transducers and activators of transcription 1 and 2 (STAT1 and STAT2). These two transcription factors are able

to form heterodimers that can bind the interferon-stimulated response element and thereby increase the expression of interferon-stimulated genes.

Several of the proteins mentioned above are chemoattractants or activators of blood monocytes, memory T helper cells, and/or eosinophils. Indeed, IL18 acts on natural killer cell activity, lymphocyte T helper 1 (Th1) interferon gamma (IFN- γ) production and Th1 cell proliferation (reviewed in ref 58). CCL5 is a chemoattractant for blood monocytes, memory T helper cells and eosinophils (45). When it binds to CXCR3, CXCL10 stimulates monocyte, natural killer cell and T-cell migration (48).

The expression of monocyte attractants in pregnant goat mammary gland suggests that macrophages and eosinophils migrate from blood to mammary tissue. This phenomenon has been already reported during mouse mammary gland development and was associated with matrix remodeling (reviewed in Ref. 21). Thus, goat mammary gland differentiation could comprise two phases of tissue remodeling, one at midpregnancy and one in the last third of pregnancy (P70 and P110), characterized by phagocytosis of one cell type (adipocytes) or stroma and development and differentiation of another cell type (epithelium). This is in line with the upregulation of genes coding for proteins involved in the ruminant mammary gland immune response to mastitis, exemplified by C1q and lactoferrin. C1q plays an essential role in the classical pathway of the complement system (46), whereas lactoferrin has been reported to be mainly expressed by the MEC lining the ducts and the cistern (35) and to function as a iron captor preventing bacterial development (46, 54). Other proteins are specific to epithelial cells, such as TLR3, which is mainly described in intestinal epithelial cells of normal mucosa (12).

The notion by which the goat mammary gland expresses a large number of innate immune genes in pregnancy is consistent with the idea developed by Vorbach et al. (61) that mammary glands originate in the innate immune system. The innate immune system, also known as nonspecific or nonimmune responsiveness, is a first line of immediate defense. This type of protection appears crucial for a tissue exposed to multiple etiological agents.

Moreover, cluster analysis of lactating goat mammary gland showed downregulation of the IL-4 signaling pathway (*metacluster E*), characterized by downregulation of the IL4R and NFATc2 genes. Proteins encoded by these genes are lymphocyte T helper 2 (Th2) cytokines that participate in mouse mammary gland development in vivo (30). Secretion of these cytokines by mouse MEC signals the induction of the differentiation process (30), and shows the role of immune cell signaling proteins in MEC fate and function (63). At 46 days of pregnancy, the goat mammary gland expresses genes of the IL-4 signaling pathway, suggesting that the differentiation process is already engaged at this stage. The decreased expression of genes encoding these proteins during lactation is consistent with the notion that the 40th days of lactation corresponds to a stage at which MEC are fully differentiated and the mammary gland does not express differentiation markers.

Taken together, these data show the increased expression in the goat mammary gland at midpregnancy of a large number of genes encoding proteins involved in the immune system, as well as milk proteins. A common regulatory pathway (or at least pathways mobilizing common effectors)

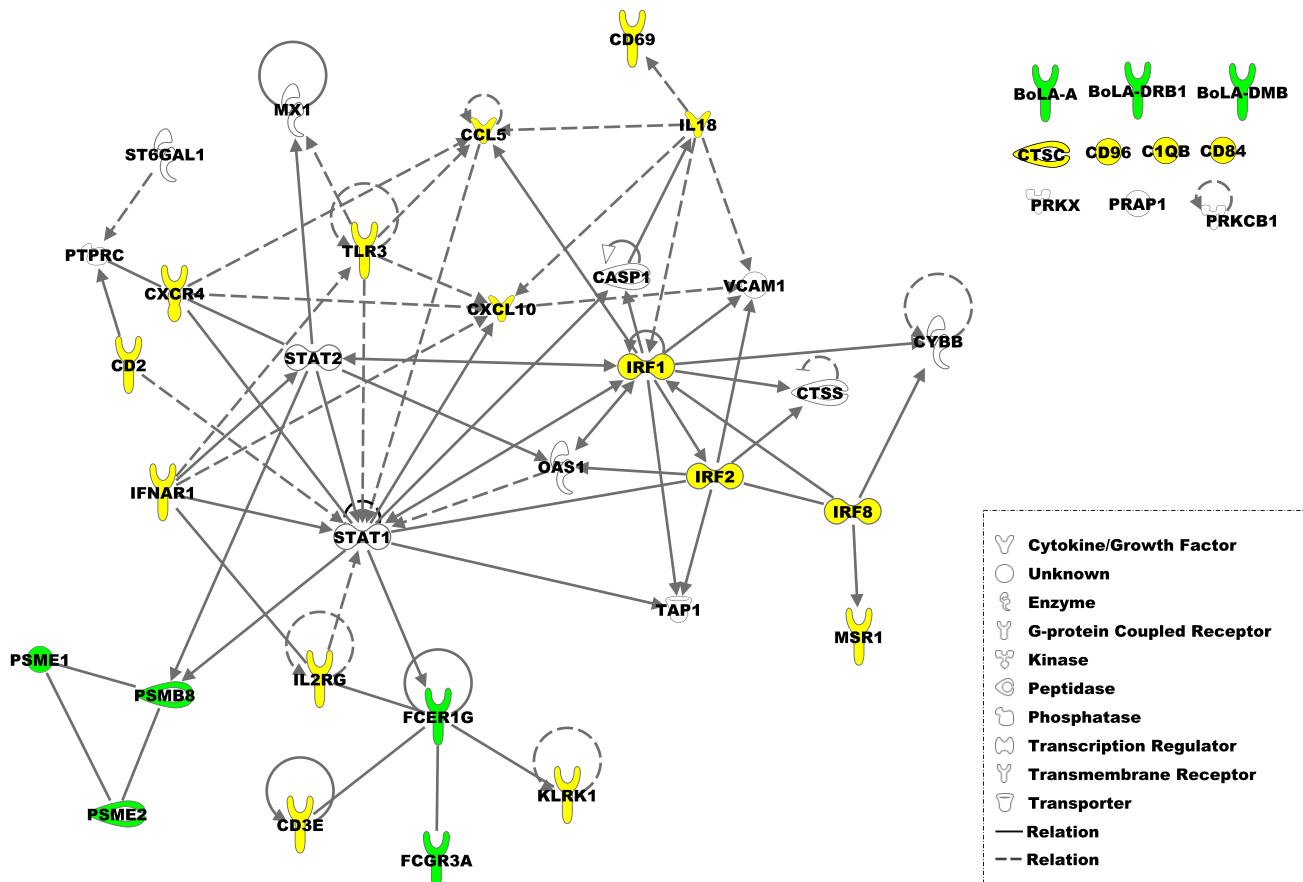


Fig. 7. Interaction networks between immune response genes with IDID expression profiles (*metacluster A*). Genes of the innate immune response are in yellow. Genes of the specific immune response are in green. BoLA-A: major histocompatibility complex, class I, A; BoLA-DMB: major histocompatibility complex, class II, DM β ; BoLA-DRB1: major histocompatibility complex, class II, DR β 1; C1QB: complement component 1, q subcomponent, B chain; CASP1: caspase 1, apoptosis-related cysteine peptidase (interleukin 1, β , convertase); CCL5: chemokine (C-C motif) ligand 5; CD2: CD2 molecule; CD3E: CD3e molecule, ϵ (CD3-TCR complex); CD69: CD69 molecule; CD84: CD84 molecule; CD96: CD96 molecule; CTSC: cathepsin C; CTSS: cathepsin S; CXCL10: chemokine (C-X-C motif) ligand 10; CXCR4: chemokine (C-X-C motif) receptor 4; CYBB: cytochrome b-245, β -polypeptide; FCER1G: Fc fragment of IgE, high affinity I, receptor for; γ -polypeptide; FCGR3A: Fc fragment of IgG, low affinity IIIa, receptor (CD16a); IFNAR1: interferon (α , β , and ω) receptor 1; IL2RG: interleukin 2 receptor, γ (severe combined immunodeficiency); IL18: interleukin 18 (interferon-gamma-inducing factor); IRF1: interferon regulatory factor 1; IRF2: interferon regulatory factor 2; IRF8: interferon regulatory factor 8; KLRK1: killer cell lectin-like receptor subfamily K, member 1; MSR1: macrophage scavenger receptor 1; MX1: myxovirus (influenza virus) resistance 1, interferon-inducible protein p78; OAS1: 2',5'-oligoadenylate synthetase 1, 40/46 kDa; PRAP1: prolin-rich acidic protein 1; PRKCB1: protein kinase C, β ; PRKX: protein kinase, X-linked; PSMB8: proteasome (prosome, macropain) subunit, β -type, 8 (large multifunctional peptidase 7); PSME1: proteasome (prosome, macropain) activator subunit 1 (PA28 α); PSME2: proteasome (prosome, macropain) activator subunit 2 (PA28 β); PTPRC: protein tyrosine phosphatase, receptor type, C; ST6GAL1: ST6 β -galactosamide α -2,6-sialyltransferase 1; STAT1: signal transducer and activator of transcription 1, 91 kDa; STAT2: signal transducer and activator of transcription 2, 113 kDa; TAP1: transporter 1, ATP-binding cassette, subfamily B (MDR/TAP); TLR3: Toll-like receptor 3; VCAM1: vascular cell adhesion molecule 1.

might thus control the expression of immune functions and milk protein genes. The increased expression of immune genes in midpregnancy supports a crucial role of immune proteins in mammary tissue development and functional differentiation.

Conclusion

With respect to the general mechanisms underlying goat mammary gland development, mammary tissue appears to switch from a stromal tissue to a lobulo-alveolar epithelium during the first half of pregnancy. This is shown by the downregulation of adipocyte-specific genes, such as adiponectin (ADIPOQ), and the upregulation of chemokine encoding genes, which are thought to attract phagocytes into the goat mammary gland where they participate in its remodeling. The second half of pregnancy is characterized by MEC proliferation.

As in several other mammals (mice, rabbits, and cows), the secretory activity of the goat mammary gland is only activated after parturition. However, as induction of the differentiation process seems to take place before 46 days of pregnancy, studies of the underlying mechanism would require earlier screening of developmental stages, during the first third of pregnancy.

Genes of immunity that are upregulated during pregnancy (mainly at P70) participate in the remodeling phase of the differentiation process. A subset of these genes is ready to be switched on and provide both the neonate intestine and the mammary tissue of the lactating goat with nonspecific immunity. As they are downregulated during lactation, immune genes expressed in mammary tissue during pregnancy appear to participate in mammary gland development and remodeling during terminal differentiation, rather than having a protective role.

Finally, this work provides the first comprehensive analysis of gene expression during functional differentiation of ruminant mammary gland, based on microarray technology. However, these data were obtained with whole, heterogeneous mammary tissues. In ruminants, the lobulo-alveolar epithelium develops within a stromal compartment composed of multiple cell types. Molecular cross talk exists between these cell compartments (epithelial and stromal), and gene expression measurements in such heterogeneous tissue makes it difficult to identify the contributions of specific cell types. In addition, they are based on weighted averages of expression levels in different cell populations, the relative abundance of which changes during pregnancy. Therefore, to precisely determine their relative contributions to the functional differentiation process, gene expression analysis should be repeated in defined cell populations. This is currently underway in our laboratory, using powerful new technologies such as laser capture microdissection.

ACKNOWLEDGMENTS

We thank the UCEA team (INRA, Centre de Recherche de Jouy-en-Josas) for taking care of the animals, Marie-Laure Martin-Magniette (AgroParisTech) for advice on the microarray experimental design, Philippe Bardoux and Cedric Cabau (SIGENAE) for help in GO data publication and gene annotation, and Karine Hugot and Diane Esquerre (CRB-GADIE) for providing the 22K bovine oligoarrays. Finally, we thank the three anonymous referees for their helpful suggestions.

DISCLOSURES

No conflicts of interest are declared by the author(s).

REFERENCES

- Akers RM. Lactational physiology: a ruminant animal perspective. *Protoplasma* 159: 96–111, 1990.
- Akers RM. Lactogenic hormones: binding sites, mammary growth, secretory cell differentiation, and milk biosynthesis in ruminants. *J Dairy Sci* 68: 501–519, 1985.
- Anderson RR, Harness JR, Snead AF, Salah MS. Mammary growth pattern in goats during pregnancy and lactation. *J Dairy Sci* 64: 427–432, 1981.
- Anderson SM, Rudolph MC, McManaman JL, Neville MC. Key stages in mammary gland development. Secretory activation in the mammary gland: it's not just about milk protein synthesis! *Breast Cancer Res* 9: 204–218, 2007.
- Atabai K, Sheppard D, Werb Z. Roles of the innate immune system in mammary gland remodeling during involution. *J Mammary Gland Biol Neoplasia* 12: 37–45, 2007.
- Baldwin RL. Enzymatic activities in mammary glands of several species. *J Dairy Sci* 49: 1533–1542, 1966.
- Benjamini Y, Hochberg Y. Controlling the false discovery rate: a practical and powerful approach to multiple testing. *J Royal Stat Soc Serie B* 47: 289–300, 1995.
- Bevilacqua C, Helbling JC, Miranda G, Martin P. Translational efficiency of casein transcripts in the mammary tissue of lactating ruminants. *Reprod Nutr Dev* 5: 567–578, 2006.
- Bionaz M, Looor JJ. Gene networks driving bovine milk fat synthesis during the lactation cycle. *BMC Genomics* 9: 366, 2008.
- Brazma A, Hingamp P, Quackenbush J, Sherlock G, Spellman P, Stoeckert C, Aach J, Ansorge W, Ball CA, Causton HC, Gaasterland T, Glenisson P, Holstege FCP, Kim IF, Markowitz V, Matese JC, Parkinson H, Robinson A, Sarkans U, Schulze-Kremer S, Stewart J, Taylor R, Vilo J, Vingron M. Minimum information about microarray experiment (MIAME) - toward standards for microarray data. *Nature Genomics* 29: 365–371, 2001.
- Capuco AV, Connor EE, Wood DL. Regulation of mammary gland sensitivity to thyroid hormones during the transition from pregnancy to lactation. *Exp Biol Med (Maywood)* 233: 1309–1314, 2008.
- Cario E, Podolsky DK. Differential alteration in intestinal epithelial cell expression of toll-like receptor 3 (TLR3) and TLR4 in inflammatory bowel disease. *Infect Immun* 68: 7010–7017, 2000.
- Cases S, Zhou P, Shillingford JM, Wiseman BS, Fish JD, Angle CS, Hennighausen L, Werb Z, Farese RV. Development of the mammary gland requires DGAT1 expression in stromal and epithelial tissues. *Development* 131: 3047–3055, 2004.
- Chanat E, Martin P, and Ollivier-Bousquet M. AlphaS1-casein is required for the efficient transport of beta-casein and kappa-casein from the endoplasmic reticulum to the Golgi apparatus mammary epithelial cells. *J Cell Sci* 112: 3399–3412, 1999.
- Choi KM, Barash I, Rhoads RE. Insulin and prolactin synergistically stimulate beta-casein messenger ribonucleic acid translation by cytoplasmic polyadenylation. *Mol Endocrinol* 18: 1670–1686, 2004.
- Clarkson RWE, Wayland MT, Lee JH, Freeman T, Watson CJ. Gene expression profiling of mammary gland development reveals putative roles for death receptors and immune mediators in post-lactational regression. *Breast Cancer Res* 6: R92–R109, 2003.
- Connor EE, Meyer MJ, Li RW, Van Amburgh ME, Boisclair YR, Capuco AV. Regulation of gene expression in the bovine mammary gland by ovarian steroids. *J Dairy Sci* 90: E55–E65, 2007.
- Delmar P, Robin S, Daudin JJ. VarMixt: efficient variance modelling for the differential analysis of replicated gene expression data. *Bioinformatics* 21: 502–508, 2005.
- Everts RE, Chavatte-Palmer P, Razzak A, Hue I, Green CA, Oliveira R, Vignon X, Rodriguez-Zas SL, Tian XC, Yang X, Renard JP, Lewin HA. Aberrant gene expression patterns in placentomes are associated with phenotypically normal and abnormal cattle cloned by somatic cell nuclear transfer. *Physiol Genomics* 33: 65–77, 2008.
- Finucane KA, McFadden TB, Pond JP, Kennelly JJ, Zhao FQ. Onset of lactation in the bovine mammary gland: gene expression profiling indicates a strong inhibition of gene expression in cell proliferation. *Funct Integr Genomics* 8: 251–264, 2008.
- Goudon-Evans V, Lin EY, Pollard JW. Requirement of macrophages and eosinophils and their cytokines/chemokines for mammary gland development. *Breast Cancer Res* 4: 155–164, 2002.
- Hennighausen L, Robinson GW. Signaling pathways in mammary gland development. *Dev Cell* 1: 467–475, 2001.
- Hennighausen L, Robinson GW. Think globally, act locally: the making of a mouse mammary gland. *Genes Dev* 12: 449–455, 1998.
- Hovey RC, McFadden TB, Akers RM. Regulation of mammary gland growth and morphogenesis by the mammary fat pad: a species comparison. *J Mammary Gland Biol Neoplasia* 4: 53–68, 1999.
- Hovey RC, Trott JF, Vonderhaar BK. Establishing a framework for the functional mammary gland: from endocrinology to morphology. *J Mammary Gland Biol Neoplasia* 7: 17–38, 2002.
- Hu E, Liang P, Spiegelman BM. AdipoQ is a novel adipose-specific gene dysregulated in obesity. *J Biol Chem* 271: 10697–10703, 1996.
- Kanazawa T, Kohmoto K. Immunohistochemical demonstration of alphaS1 and beta casein in mouse mammary glands at early stages of pregnancy. *J Histochem Cytochem* 50: 257–264, 2002.
- Kerr MK. Design considerations for efficient and effective microarray studies. *Biometrics* 59: 822–828, 2003.
- Kerr MK, Churchill GA. Experimental design for gene expression microarrays. *Biostatistics* 2: 183–201, 2001.
- Khaled WT, Read EKC, Nicholson SE, Baxter FO, Brennan AJ, Came PJ, Sprigg N, McKenzie ANJ, Watson CJ. The IL-4/IL-13/Stat6 signalling pathway promotes luminal mammary epithelial cell development. *Development* 134: 2739–2750, 2007.
- Mary-Huard T, Picard F, Robin S. Introduction to statistical methods for microarray data analysis. In: *Mathematical and Computational Methods in Biology*, edited by Hermann. Paris: 2006, p. 56–126.
- Master SR, Hartman JL, D'Cruz CM, Moody SE, Keiper EA, Ha SI, Cox JD, Belka GK, Chodosh LA. Functional microarray analysis of mammary organogenesis reveals a developmental role in adaptive thermogenesis. *Mol Endocrinol* 16: 1185–1203, 2002.
- Mellenberger RW, Bauman DE. Metabolic adaptations during lactogenesis. Fatty acid synthesis in rabbit mammary tissue during pregnancy and lactation. *Biochem J* 138: 373–379, 1974.
- Mellenberger RW, Bauman DE, Nelson DR. Metabolic adaptations during lactogenesis. Fatty acid and lactose synthesis in cow mammary tissue. *Biochem J* 136: 741–748, 1973.
- Molenaar AJ, Kuys YM, Davis SR, Wilkins RJ, Mead PE, Tweedie JW. Elevation of lactoferrin gene expression in developing, ductal, rest-

- ing, and regressing parenchymal epithelium of the ruminant mammary gland. *J Dairy Sci* 79: 1198–1208, 1996.
36. Mori S, Nishikawa SI, Yokota Y. Lactation defect in mice lacking the helix-loop-helix inhibitor Id2. *EMBO J* 19: 5772–5781, 2000.
 37. Nakhasi HL, Qasba PK. Quantitation of milk proteins and their mRNAs in rat mammary gland at various stages of gestation and lactation. *J Biol Chem* 254: 69016–66025, 1979.
 38. Naylor MJ, Oakes SR, Gardiner-Garden M, Harris J, Blazek K, Ho TWC, Li FC, Wynick D, Walker AM, Ormandy CJ. Transcriptional changes underlying the secretory activation phase of mammary gland development. *Mol Endocrinol* 19: 1868–1883, 2005.
 39. Neville MC, McFadden TB, Forsyth I. Hormonal regulation of mammary differentiation and milk secretion. *J Mammary Gland Biol Neoplasia* 7:49–66, 2002.
 40. Niranjana B, Buluwela L, Yant J, Perusinghe N, Atherton A, Phippard D, Dale T, Gusterson B, Kamalati T. HGF/SF: a potent cytokine for mammary growth, morphogenesis and development. *Development* 121: 2897–2908, 1995.
 41. Ogg SL, Weldon AK, Dobbie L, Smith AJH, Mather IH. Expression of butyrophilin (Btln1) in lactating mammary gland is essential for the regulated secretion of milk lipid droplets. *Proc Natl Acad Sci USA* 101: 10084–10089, 2004.
 42. Ollier S, Robert-Granié C, Bernard L, Chilliard Y, Leroux C. Mammary transcriptome analysis of food-deprived lactating goats highlights genes involved in milk secretion and programmed cell death. *J Nutr* 137: 560–567, 2007.
 43. Pedchenko VK, Imagawa W. Pattern of expression of the KGF receptor and its ligands KGF and FGF-10 during postnatal mouse mammary gland development. *Mol Reprod Dev* 56: 441–447, 2000.
 44. Pitelka DR, Hamamoto ST, Duafala JG, Nemanic MK. Cell contacts in the mouse mammary gland - Normal gland in postnatal development. *J Cell Biol* 56: 797–818, 1973.
 45. Proudfoot AEI, Buser R, Borlat F, Alouani S, Soler D, Offord RE, Schroder JM, Power CA, Wells TNC. Amino-terminally modified RANTES analogues demonstrate differential effects on RANTES receptors. *J Biol Chem* 274: 32478–32485, 1999.
 46. Rainard P, Riollet C. Innate immunity of the bovine mammary gland. *Vet Res* 37: 369–400, 2006.
 47. Robinson GW, McKnight RA, Smith GH, Hennighausen L. Mammary epithelial cells undergo secretory differentiation in cycling virgins but require pregnancy for the establishment of terminal differentiation. *Development* 121: 2079–2090, 1995.
 48. Romagnani P, Annunziato F, Lazzeri E, Cosmi L, Beltrame CL, L, Galli G, Francalanci M, Manetti R, Marra F, Vanini V, Maggi E, Romagnani S. Interferon-inducible protein 10, monokine induced by interferon gamma, and interferon-inducible T-cell alpha chemoattractant are produced by thymic epithelial cells and attract T-cell receptor (TCR) alpha beta+ CD8+ single-positive T cells, TCR gamma delta+ T cells, and natural killer-type cells in human thymus. *Blood* 97: 601–607, 2001.
 49. Rudolph MC, McManaman JL, Hunter L, Phang T, Neville MC. Functional development of the mammary gland: use of expression profiling and trajectory clustering to reveal changes in gene expression during pregnancy, lactation, and involution. *J Mammary Gland Biol Neoplasia* 8: 287–307, 2003.
 50. Rudolph MC, McManaman JL, Phang TL, Russell T, Kominsky DJ, Serkova NJ, Anderson SM, Neville MC. Metabolic regulation in the lactating mammary gland: a lipid synthesizing machine. *Physiol Genomics* 28: 323–336, 2007.
 51. Saeed AI, Sharov V, White J, Li J, Liang W, Bhagabati N, Braisted J, Klapa M, Currier T, Thiagarajan M, Sturn A, Snuffin M, Rezantsev A, Popov D, Ryltsov A, Kostukovich E, Borisovsky I, Liu Z, Vinsavich A, Trush V, Quackenbush J. TM4: a free, open-source system for microarray data management and analysis. *Biotechniques* 34: 374–378, 2003.
 52. Schroeder A, Mueller O, Stocker S, Salowsky R, Leiber M, Fgasmann M, Lightfoot S, Menzel W, Granzow M, Ragg T. The RIN: an RNA integrity number for assigning integrity values to RNA measurements. *BMC Molecular Biology* 7: 3, 2006.
 53. Schwertfeger KL, McManaman JL, Palmer CA, Neville MC, Anderson SM. Expression of constitutively activated Akt in the mammary gland leads to excess lipid synthesis during pregnancy and lactation. *J Lipid Res* 44: 1100–1112, 2003.
 54. Sordillo LM, Streicher KL. Mammary gland immunity and mastitis susceptibility. *J Mammary Gland Biol Neoplasia* 7: 135–146, 2002.
 55. Soukas A, Cohen P, Socci ND, Friedman JM. Leptin-specific patterns of gene expression in white adipose tissue. *Genes Dev* 14: 963–980, 2000.
 56. Stein T, Morris JS, Davies CR, Weber-Hall SJ, Duffy MA, Heath VJ, Bell AK, Ferrier RK, Sandilands GP, Gusterson BA. Involution of the mouse mammary gland is associated with an immune cascade and an acute-phase response, involving LBP, CD14 and STAT3. *Breast Cancer Res* 6: R75–R91, 2004.
 57. Suchyta SP, Sipkovsky S, Halgren RG, Kruska R, Elftman M, Weber-Nielsen M, Vandelaar MJ, Xiao L, Tempelman RJ, Coussens PM. Bovine mammary gene expression profiling using a cDNA microarray enhanced for mammary-specific transcripts. *Physiol Genomics* 16: 8–18, 2003.
 58. Suzuki N, Chen NJ, Millar DG, Suzuki S, Horacek T, Hara H, Bouchard D, Nakanishi K, Penninger JM, Ohashi PS, Yeh WC. IL-1 receptor associated kinase 4 is essential for IL-18 mediated NK and Th1 cell responses. *J Immunol* 170: 4031–4035, 2003.
 59. Swanson EW, Poffenbarger JL. Mammary gland development of dairy heifers during their first gestation. *J Dairy Sci* 62: 702–714, 1979.
 60. Tucker HA. Hormone, mammary growth, lactation: a 41-year perspective. *J Dairy Sci* 83: 874–884, 2000.
 61. Vorbach C, Capecchi MR, Penninger JM. Evolution of the mammary gland from the innate immune system? *Bioessays* 28: 606–616, 2006.
 62. Wang M, Master SR, Chodosh LA. Computational expression deconvolution in a complex mammalian organ. *BMC Informatics* 7: 328, 2006.
 63. Watson CJ. Immune cell regulators in mouse mammary development and involution. *J Anim Sci* 87, Suppl: 35–42, 2008.
 64. Yang Y, Dudoit S, Luu D, Peng V, Ngai J, Speed T. Normalization for cDNA microarray data: a robust composite method addressing single and multiple slide systematic variation. *Nucleic Acids Res* 30: e15, 2002.